



# **The Search for Exoplanets**

*A Major Qualifying Project*

*Submitted by:*

**Christian J. Iamartino**

*To the faculty of:*

**Worcester Polytechnic Institute**

*In partial fulfillment of the requirements for the degree of:*

**Bachelor of Science**

*For the department of:*

**PHYSICS**

*Advised by:*

**P.K. Aravind**



*September 25, 2014*



## Table of Contents

|  |    |
|--|----|
| 1. Abstract.....   | 4  |
| 2. Motivation.....   | 5  |
| 3. Project Objectives .....  | 6  |
| 4. Introduction.....   | 7  |
| 4.1 What are Exoplanets? .....   | 7  |
| 4.2 Why Search for Them? .....   | 8  |
| 4.3 A Brief History of Exoplanets, From Antiquity to Modern Times..... | 9  |
| 4.3.1 Origins of the Planetary Sciences .....                          | 9  |
| 4.3.2 The Emergence and Development of Exoplanetary Studies.....       | 13 |
| 4.4 Discovered at Last, The Case of PSR 1257+12.....                   | 17 |
| 4.5 Notable Findings in the Field of Exoplanets Since 1992.....        | 19 |
| 5. Technical Background .....  | 21 |
| 5.1 Principal Methods for the Detection of Exoplanets .....            | 21 |
| 5.1.1 The Radial Velocity Method.....                                  | 22 |
| 5.1.2 The Transit Method.....  | 25 |
| 5.2 Other Methods for the Detection of Exoplanets .....                | 34 |
| 5.2.1 The Pulsar Timing Method .....                                   | 34 |
| 5.2.2 The Gravitational Lensing Method .....                           | 35 |
| 5.2.3 The Direct Observation Method .....                              | 36 |
| 5.2.4 The Astrometric Method.....                                      | 37 |
| 6. Statistics of Current Exoplanet Discoveries.....                    | 38 |
| 6.1 Goals .....  | 38 |
| 6.2 Sources.....   | 38 |
| 6.3 Data Analysis.....   | 40 |
| 6.3.1 Exoplanetary System Characteristics.....                         | 40 |
| 6.4 Summary of Findings.....   | 41 |
| 6.4.1 What kinds of stars do these planets form around?.....           | 41 |
| 6.3.2 Where are these exoplanets located?.....                         | 43 |
| 7. Detecting an Exoplanet.....   | 44 |
| 7.1 Candidate Selection .....  | 44 |
| 7.2 Location and Equipment.....  | 46 |
| 7.3 Image Capture and Processing.....                                  | 49 |
| 7.4 Observation Night and Measured Light Curve .....                   | 51 |

|   |    |
|---|----|
| 7.5 Summary of Findings.....                          | 52 |
| 8. Summary and Conclusion .....                       | 54 |
| 9. Appendices.....                                    | 55 |
| 9.1 Appendix A – Stellar Development .....            | 55 |
| 9.2 Appendix B – Stellar Classification Systems ..... | 58 |
| Spectral Classes .....                                | 58 |
| The Hertzsprung-Russel Diagram .....                  | 59 |
| Peculiarities in the Hertzsprung-Russel Diagram ..... | 60 |
| 9.3 Appendix C: Excel Algorithms.....                 | 62 |
| 10. Acknowledgements.....                             | 63 |
| Table of Figures .....                                | 64 |
| References.....                                       | 67 |

## 1. Abstract

The study of exoplanets is an emerging field of astrophysics which endeavors to locate and study planets outside of our Solar System. Since the discovery of PSR1257+12 b in 1992, nearly a thousand extrasolar planets have been confirmed and carefully examined, vastly expanding our knowledge of the planetary sciences and the universe as a whole. This project primarily develops an overarching understanding of the physics and history behind the development of the exoplanetary sciences, including an analysis of the trends found in the current list of exoplanetary discoveries. With a specific focus and examination of the transit method, this project also provides a summary of data gathered from a live observation of the exoplanet WASP-13 b, observed on the evening of April 2, 2013.

## 2. Motivation

The motivation for this project arises from an intense personal and academic interest in the fields of stellar astrophysics and the planetary sciences. With the upsurge of recent popular interest in finding the ever-elusive “second-Earth”, a discovery that is by the day growing tantalizingly nearer, I felt that stepping back to take in the greater picture of the current discoveries might be useful to both myself, and to future observers. In the end, I hope to come out of this project with a greater appreciation and understanding of “The Search for Exoplanets”, and to set a solid groundwork for my own future exoplanetary studies.

### 3. Project Objectives

Three principal objectives were identified at the onset of project work. These objectives were defined to provide a clear progression of development of the project, and are listed below.

**Stage 1** Defined the period under which a general overview of the exoplanetary sciences was conducted. The goal of this stage was to gain a comprehensive understanding of the history, development, and current techniques used by astronomers and astrophysicists to detect exoplanets, with a special focus on the transit method. This provided the necessary scientific background to commence with the next two stages of the project.

**Stage 2** Defined the period during which the information gathered in Stage 1 was used to analyze the current data on exoplanetary findings. With this information, we were able to gain an extensive understanding of the important trends to be found in the types of exoplanets that have currently been discovered, along with important characteristics on transiting exoplanets that would play into our investigation in the third and final stage.

**Stage 3** Defined the period where the information gathered in Stages 1 and 2 fed into our real-world investigation and detection of an exoplanet using the astronomical equipment located at the Olmsted Observatory in Pomfret, Connecticut. It is hoped that the knowledge and experience gained from this stage of the project will be of use in future endeavors, and also prove as a testing ground for a new sky survey to be developed and continued in the future.

## 4. Introduction

### 4.1 What are Exoplanets?

In simple terms, the word “exoplanet” (sometimes rendered as “extrasolar planet”) refers to a planetary body that exists outside of the boundaries of our Solar System. The name ultimately derives from the Greek *εξώ*, meaning “outside”, and *πλανήτης*, meaning “planet”, and was coined in the early 1990s. Exoplanets come in a wide variety of sizes and compositions - some being large gas giants like Jupiter or Saturn, while others are small and rocky, like Earth and Mars. Exoplanets are almost always found to be gravitationally bound to a stellar system, however, there is at least some evidence to suggest that there may be a small minority of “rogue exoplanets” that roam the interstellar void, unbound to any one system. As of September 2014, astronomers have discovered nearly one thousand confirmed exoplanets, with several thousand more unconfirmed. Yet even with this seemingly small number compared to the hundred billion stars in our galaxy, we have already learned that planets are certainly not as rare as once thought.

## 4.2 Why Search for Them?

One of the main reasons for studying exoplanets is the fact that they allow astronomers and astrophysicists the chance to observe planetary systems that have developed independently of our own Solar System. This seemingly mundane point has arguably been the source of some of the greatest questions that humanity has produced, including the holy grail of questions: “are we the only ones out here?”. Indeed, although we, as humans, have gained a vast amount of knowledge about the thousands of planets and planetisimals that inhabit our Solar System, the common origin of these bodies is inherently limiting, for, as we have seen through our observations of other stellar systems, not all stars are made equally, nor are the nebulae from which they are formed made of the same materials. Therefore, when we observe all of the bodies that inhabit our Solar System, we are looking only at *a single microcosm* in the vast expanse of the greater cosmos. Naturally, we must observe other star systems to gain a better understanding of the common functions of stellar and planetary systems throughout our galaxy, and the universe.

By observing exoplanets, and making note of their composition, size, orbital parameters, and the stars which they form around, we gain an understanding of the various conditions under which planets may form. Although we have discovered only a thousand planets of a myriad of possible ones that exist in our galaxy and beyond, our understanding of these thousand have already greatly furthered our understanding of the laws of planetary systems – the same laws that must govern planetary formation throughout the universe. In time, as more and more planets are discovered and added to our databases, we may ultimately be able to understand the ideal conditions which allow for planets like Earth to form. And from this, we may even be able to predict which stars will be most likely to harbor other Earths.

## 4.3 A Brief History of Exoplanets, From Antiquity to Modern Times

### 4.3.1 Origins of the Planetary Sciences

The exoplanetary sciences have their origins in antiquity, when ancient astronomers first began to write down theories regarding the regular motions of strange moving “stars” in the sky. To the Ancient Greeks, each wandering “star” became known as a *πλανήτης*, which in their tongue meant “wanderer”, and these objects were continually a source of discussion amongst ancient peoples all over the world. Aristotle, one of the first philosophers to write on the subject, stated:

*As to the position of the earth, then, this is the view which some advance, and the views advanced concerning its rest or motion are similar. For here too there is no general agreement. All who deny that the earth lies at the center think that it revolves about the center, and not the earth only but, as we said before, the counter-earth as well. Some of them even consider it possible that there are several bodies so moving, which are invisible to us owing to the interposition of the earth. This, they say, accounts for the fact that eclipses of the moon are more frequent than eclipses of the sun: for in addition to the earth each of these moving bodies can obstruct it.*<sup>1</sup>

However, while much thought and study was given to the motions of these strange objects, and much information was gathered regarding their supposed nature, ultimately, ancient science was incapable of explaining exactly what these planets were or how they moved.

One of the first people to formalize their theories regarding the movements of the planets was Claudius Ptolemy, a First Century Roman astronomer from Egypt, who wrote a monumental tome titled *The Almagest*, which built upon centuries of work conducted by the natural philosophers of Greece, Rome, Persia, and perhaps even India as well. In his work, Ptolemy outlined a Geo-centric (meaning “Earth-centered”) theory which ascribed the motions of the mysterious planets to a path of motion which he called an epicycle, meaning “exterior circle”. Planets under his model orbited the center of the epicycle, which in turn orbited around the Earth in a perfectly circular path known as a deferent. In this manner, Ptolemy, and many of his

---

<sup>1</sup>Aristotle, *On the Heavens*

contemporaries, believed that there was now a proper explanation for the mysterious motion of the wayward stars.

However, Ptolemy's system, which remained the standard model of the universe in the West for nearly a thousand years, was flawed. One critical piece of evidence that his work mostly failed to explain was the planetary "retrograde motion", that is, the reason for why the planets seemed to "backtrack" in an S-shape on their path across the celestial hemisphere. Ptolemy's theory originally had set out to explain this problem in a concrete way, which was something that his predecessors, namely Aristotle and Hipparchos, had failed to do. But even with this well-defined goal in mind, Ptolemy's theories presented many problems for the scientists who followed in his footsteps. For centuries, these followers grappled with the question of why the epicycles and deferents did not line up properly with their observations. In an attempt solve these glaring issues, the scholars of Late Antiquity developed increasingly complex and inelegant systems involving, spirals, tangents, and arcs, desperately trying to explain the problems inherent in the *Almagest*, but, for many centuries, no one was found to be capable of resolving the issues.

With the political instability and ultimate decline of central authority in the Roman world in the 5<sup>th</sup> – 7<sup>th</sup> Centuries (the end of Late Antiquity), detailed analyses of Ptolemy's model slowed to a crawl in the West. During this era, the new Church Ecumenical Councils that decided the fate of the now deeply religious Christianized Roman Empire had forced religious leaders and Roman citizens to promote a viewpoint, based on the theories of both Aristotle and Ptolemy, of a permanent, unmutable, geo-centric universe of "God's heavenly spheres". Unfortunately, despite the benefit of greater unity within the new state religion of the Late Roman Empire, these definitive Ecumenical decisions, heavily enforced by the Romano-Byzantine Emperors of the era, severely limited further breakthroughs regarding Ptolemy's problematic model. Anyone who openly challenged the viewpoint of the Church and State was summarily suppressed. It would take several centuries of war, famine, chaos, and finally, political, religious, and social upheaval, for the flaws inherent in Ptolemy's *Almagest* to finally have the chance to be corrected.

However, around the same time that the advancement of astronomical knowledge in the Western world ground to a halt, a keen interest in astronomy took hold in the East. Starting in the mid 500s in India, famous astronomers such as Arhabyata and Brahmagupta made great strides in the understanding of celestial phenomena, including the notion that the moon shone brightly because

of reflected sunlight, and several new theories regarding the motions of the planets. Due to the destruction of the Sassanid Persian state at the hands of the Arabs in the 630s, it is likely that the much praised astronomical knowledge of the Arab world had its beginnings from this golden age of Indian astronomy. As links between the East and West grew with the development of the Silk Road and Spice Trade from China and India to the West during the period, many of the ideas that originated in India made their way into Arabia and Persia, and finally, into Europe.

During the 8<sup>th</sup> and 9<sup>th</sup> Centuries, the Arab world benefitted greatly from an influx of ancient texts from many sources across the known world. Not only did they receive the previously-mentioned Indian and Persian texts from the demise of the Sassanids, but following a ceasefire with the Byzantine Emperor Theophilos, the Caliph al-Mamun requested Byzantine copies of the works of the ancient Greek and Roman philosophers, including Ptolemy's *Almagest*. Following this exchange, the Arab world, particularly the capital at Baghdad, became renowned for its scientific achievements. Astronomy, optics, and mathematics, became widely studied, and intellectual exchanges between the Muslim and Byzantine world became common, to the benefit of both.

From the 10<sup>th</sup> through 12<sup>th</sup> Centuries, with the stabilization of the Byzantine state came a new golden age of intellectualism in the Empire that began under the Macedonian Emperors and continued under the Komnenos family. Political fragmentation in the Muslim world may have hindered scientific inquiry in some locations, but, on the whole it seems that scientific investigation continued at significant levels, and scientific correspondence between Arab/Persian and Byzantine scholars seems to have flourished.

In Byzantium in particular, scholars such as Michael Psellos and Anna Komnene came to be considered the leading scientific experts of their day, and had amassed a great deal of knowledge of astronomy. It is evident from the works of these intellectuals that around this time (c.1050 – 1150) a paradigm shift had occurred in Byzantine thought that promoted what might be considered a proto scientific method - that is, that observed phenomena arose from some natural cause (and not one of the occult or supernatural), and that the way to understand these natural phenomena was through the recording of repeatable evidence. It is apparent that during this “golden age” of intellectualism in Byzantium and the Near East, Ptolemy's unchallenged position as described in *the Almagest* and the Church Councils had started to erode. Indeed, Anna Komnene's detailed and erudite descriptions of comets, stars, and planets in her

magisterial work *the Alexiad*, tells us that major strides had been made in understanding the cosmos during her time. There is even evidence to support the idea that heliocentrism may have been discussed by other leading Byzantine scholars of the day, most notably John Italos, over four centuries before Copernicus.

Yet, sadly, this era of intellectualism did not last. After nearly two centuries of significant development, the “golden ages” of both the Empire and Caliphate were abruptly extinguished with the Sack of Constantinople in AD 1204 by the Crusaders of the Fourth Crusade, and soon after, the Sack of Baghdad in AD 1258 by the Mongols. And yet, for all of the works that were burned in the Great Libraries of Constantinople and the Houses of Learning in Baghdad, one major idea survived – that Ptolemy’s “perfect model”, long the “absolute of the universe”, unable to be challenged, had finally been tarnished by the developments made by Byzantine, Arab, Persian, and Indian scholars. Whether by luck or misfortune, it was now the West’s turn to take up the banner of intellectualism and finally put to rest the question of the motion of the planets. But it would take another three centuries for this to solidly manifest itself within Western minds.

By the mid-1400s, Western Europe’s economic and social recovery following the devastating effects of the Black Death a century earlier left it in a prime position to pick up where their Byzantine predecessors had left off. An extreme interest in the works of the ancients, brought about by the Italian Renaissance (itself brought about due to centuries of trading to the East, and perhaps most importantly, the Byzantine diaspora following the Fall of the Empire in AD 1453/1461), caused the development of the humanist sentiment, which naturally found itself at odds with the teachings of the Church. Although considered dangerous and even heretical, these new humanist sentiments promoted a more grounded understanding of physical phenomena, and naturally, the humanist scholars of the era sought to explain things in more scientific, rather than spiritual, terms. Various controversies regarding the Church’s temporal authority and the investiture crises eventually led to widespread distrust of the Pope’s power and authority in all matters of life. And naturally, it was this distrust that turned people away from “faith” and more towards the reason which governs our understanding of science today.

In the wake of the Protestant Reformation, which began in 1519, several notable astronomers began to turn their eyes back onto the question of planetary orbits. Of these, by far the most famous is Nicolas Copernicus, who supported and eventually published his life’s work *De*

*Revolutionibus Orbium Coelestium*, which included his new theory of Heliocentrism – that is, the idea that the Sun, and not the Earth was the center of the universe. Despite several notable predecessors in Ancient Greece, Byzantium, Persia, and India, Copernicus’ work was what ultimately revolutionized the Western understanding of the Solar System and which allowed later astronomers to make great strides in the measurement and understanding of the planets. It was through Copernicus’ efforts that modern historians attribute the beginning of the Scientific Revolution in Europe.

Thirty years after the death of Copernicus (c. 1573), Tycho Brahe, a Danish noble living in what is now present-day Sweden, published his own work on *novae* that supported Copernicus’ views that the universe was not unchanging, but Brahe still believed that the Earth was the center of the universe (which shows how reluctant people were to abandon the Ptolemaic model, nearly 1400 years after *the Almagest* had been published). This belief was developed as Brahe’s own *Tychonian* model. However, while Brahe’s theories on the structure of the universe were not quite correct, his observations of the planets, taken at an open-sky observatory on the island of Hven, were used by his protégé, Johannes Kepler, in developing the latter’s monumental laws of planetary motion, physical laws that are still in use today. It is at this point in history, that the development of the telescope by Galileo and his contemporaries allowed astronomers vastly greater abilities to explore and understand the heavens – moreso than at any point in previous history. From then on, the realm of planetary studies finally became a formal, and very real field of study within the realm of the natural sciences, and grew to become one of the most prominent areas of study during the Enlightenment.

#### **4.3.2 The Emergence and Development of Exoplanetary Studies**

Around the time of Copernicus, Brahe, Kepler, and Galileo, stirrings within philosophical, theological, and scientific circles began to bring up the question of whether the Earth and the planets were the only bodies that existed within the universe. These early modern thinkers surmised that since there existed a variety of objects that orbited the Sun, that naturally, it might be possible that other spheres might exist beyond the known system of planets in proximity to

the Earth and the Sun. Writing in 1584, the Italian philosopher-astronomer Giordano Bruno recorded one of the first written statements regarding the existence of extrasolar planets, stating:

*There are countless suns and countless earths all rotating round their suns in exactly the same way as the seven planets of our system. We see only the suns because they are the largest bodies and are luminous, but their planets remain invisible to us because they are smaller and non-luminous. The countless worlds in the universe are no worse and no less inhabited than our earth.<sup>2</sup>*

Despite the fact that Bruno was burned at the stake for supposed heresy, his statements regarding the existence of other worlds seems to have inspired the leading scholars of the day. Indeed, Galileo, a contemporary of Bruno, naturally believed in a heliocentric system, and also likely harbored a fascination with the idea that there might be worlds that existed outside of the Solar System. Galileo's experiments on gravity and kinematics set the stage for further development of what we would consider today as "modern physics". Sadly, Galileo's forceful and vehement rhetoric got him into trouble with the Church, which ultimately tried him for heresy, and confined him to house arrest for the remainder of his life. However, despite this, Galileo continued to make monumental strides in the fields of optics, astronomy, and kinematics.

Yet, it would be an Englishman, Sir Isaac Newton, who would further Galileo's work and ultimately solidify the development of modern physics with the monumental work titled *Philosophiæ Naturalis Principia Mathematica*, known today as simply *Principia*, the first formal work defining the basic principles of what one would consider modern physics. Especially pertinent to the development of exoplanetary science, Newton argued for the existence of "similar systems of similar design" throughout the universe, a clear continuation of the arguments derived from the Italian Renaissance.

Throughout the 18<sup>th</sup> Century, a solidification of the models governing the motion of the planets, the discovery of two new planets, Uranus and Neptune, as well as a number of large moons

---

<sup>2</sup> Giordano Bruno, *De L'infinito Universo e Mondi*

orbiting the known planets, filled in gaps in understanding of our Solar System. By the late 1700s and early 1800s, astronomers had seemingly developed a sufficient model of the Solar System to be able to focus on new frontiers within the realms of astronomy.

Around 1775, Sir William Herschel, a German-British astronomer, (and the discoverer of the planet Uranus in 1781) began a series of groundbreaking studies on binary stars, long an obscure realm of study that hinged on Newton's theory of gravity as presented in *Principia* - still, over a century after its publishing, a hotly debated topic. Herschel sought to prove the idea that two, or even more stars could orbit in gravitationally bound systems which could be modelled by Newton's laws of gravitation. In order to prove his hypothesis, Herschel observed and recorded the motions of over 800 star systems using his signature Newtonian reflector telescope. Perhaps most pertinent to the development of exoplanetary science, Herschel in particular studied the nearby binary star system 70 Ophiuchi, recording a great deal of data including parallax and magnitude measurements. During his studies of the system, Herschel concluded that the system was indeed gravitationally bound, consisting of two stars orbiting a common barycenter. However, while he could not definitively prove it with the equipment of the time, Herschel wrote down that "a possible third, unseen companion" might also exist orbiting within the system, an idea which was based on anomalous discrepancies found in the stars' orbits that were left unaccounted for. Although never proven, this mysterious unseen companion of 70 Ophiuchi was pursued, albeit unsuccessfully, by astronomers throughout the 19<sup>th</sup> and early 20<sup>th</sup> Centuries searching for proof of the existence of planets outside of the solar system.

In the 20<sup>th</sup> Century, with the development of Edwin Hubble's theory regarding "island universes", that is other galaxies like our own, as well as the "Mars craze", fuelled by Giovanni Schiaparelli's "discovery" of canals on Mars, increased widespread interest in the planetary sciences and alien life to an unprecedented high. Additionally, the emergence of numerous science fiction novels in the early 20<sup>th</sup> Century sought to place in the public consciousness the very real possibility that extrasolar planets existed within our galaxy, and more importantly, harbored life.

Despite little concrete evidence for the existence of exoplanets around these distant stars, fervent searches for the ever-elusive extrasolar planets continued throughout the 20<sup>th</sup> Century. By 1950, many unconfirmed reports emerged from various sources of the discovery of exoplanets orbiting

both 70 Ophiuchi (the candidate mentioned by Herschel nearly 200 years prior), as well as the nearby Barnard's Star, at only 5.9 light years away, but subsequent investigations yielded nothing. Still however, hopes remained high. It was merely a lack of sophisticated computer imaging and astrometric equipment that prevented astronomers from gathering the concrete data they needed to prove the existence of exoplanets once and for all.

However, the computer revolution starting in the 1980s changed all that. With the use of advanced computer aided telescopes, and sophisticated image-capturing technology and software, it was simply a matter of time before exoplanets starting popping up on the radar. Yet, for almost ten years after the advent of advanced computer-aided telescopes, exoplanets remained elusive, and for a time, many astronomers still cast doubts as to their existence. However, in 1992, after thousands of years of the development of the planetary sciences, the answer which had been sought for so long was finally brought to light. The existence of exoplanets had finally been proven.

#### 4.4 Discovered at Last, The Case of PSR 1257+12

According to the assumptions made by astronomers in the mid-20<sup>th</sup> Century, exoplanetary systems could only arise under the conditions presented by the evolution of low-mass main sequence stars. The rationale behind this theory was that stars with large masses would not have significant time to produce complex planetary systems or would destroy any such systems with their powerful solar winds, while stars that were too small would be produced from protostellar nebulae that did not contain enough material to form extra planetary bodies. Yet, in a great irony, the first two exoplanets ever confirmed were *not* found orbiting a main sequence star at all, but orbiting the remnant of a supergiant star.

In 1992, during a survey of millisecond pulsars located at high galactic inclinations, PSR 1257+12, a rapidly spinning pulsar located nearly 1,000 light years away in the constellation Virgo, came under the radar of astronomers at the famous Arecibo Radio Telescope in Puerto Rico. Upon close examination of graphs of the pulsar's pulse profile and timing parameters, an extremely peculiar signature deviation in the regular pulsation of the star was detected. Puzzled, the astronomers began closer examination of the pulse curve for clues as to the origin of the deviation. By using a model fitting program, and additional long-period verification measurements of the pulsar's pulse curves, it was determined that there was a mysterious, "quasi-periodic wandering" of the sinusoidal periodicity of the pulsar's output ID curve. From further analysis, it was finally determined, via a least-squares fitting method and an orbital simulation, that the root cause of this irregular wandering was produced by the presence of two planets within the system. The gravitational influence of these planets caused the pulsar to "wobble", slightly distorting its pulse curve and this is what eventually allowed astronomers to estimate the physical parameters of the orbiting planets.

According to the original paper, and subsequent studies, planets PSR 1257+12 b and c are believed to be "secondary formation planets", that is, having been formed after the destruction of the star that produced the pulsar PSR 1257+12. These planets likely coalesced and formed from the planetary nebulae produced when PSR 1257+12's parent star shed its outer layers in its final death throes. In this regard, the PSR 1257+12 system was an eye-opener to astronomers, because it proved that the long-standing theoretical limitation that planets could only form around low-

mass main-sequence stars was patently false. The discovery of two planets that so clearly formed under such extreme and seemingly bizarre conditions was living proof that the “ideal” conditions for forming planets were far more varied than were previously thought. Contrary to the growing skepticism that existed prior to the discovery of these two exoplanets, it was finally shown that the population of exoplanets, a key component in the famous Drake equation promoted in the 1970s, was potentially numerous. By this fluke discovery, the fervent search for exoplanets had been single-handedly launched. In the following decade, thousands of astronomers turned their attention to exoplanetary studies, leading to the discovery of hundreds of new exoplanets.

## 4.5 Notable Findings in the Field of Exoplanets Since 1992

Since the confirmation of the PSR 1257+12 planetary system in 1992, many new and enlightening discoveries in the field of exoplanets have been made, continually expanding our knowledge of the field of exoplanets and the planetary sciences as a whole. Some of the most notable discoveries are expanded upon below.

51 Pegasi b, the first exoplanet discovered around a main sequence star, was found by Michael Mayor and Didier Queloz using the ELODIE spectrograph at the Geneva Observatory in Sauverny, Switzerland. The official report, like that of PSR 1257+12, was published in a *Nature* article titled “A Jupiter mass companion to a solar-type star” in October of 1995. 51 Pegasi, in addition to being the first exoplanet found around a typical, main sequence star, is also notable for being the first exoplanet found using the radial velocity method, and also the first planet of its type considered to be of the major class of gaseous exoplanets known as “hot Jupiters”.<sup>3</sup>

Upsilon Andromedae b and c, the first multi-exoplanetary system discovered around a main-sequence star, was first studied in 1996 by the California and Carnegie Planet Search team, led by exoplanet legend Geoff Marcy, using the Keck Observatory in Hawaii. The findings were published in the 1997 edition of the *Astrophysical Journal* in an article titled "Three New 51 Pegasi-Type Planets". The findings of the paper elaborated on three of the so-called “hot Jupiters”, first found when observing the aforementioned 51 Pegasi system. Since then, two additional planets have been discovered orbiting Upsilon Andromedae, and the system is also marked for further observation in the hopes of discovering elusive terrestrial exoplanets.<sup>4</sup>

The discovery of Gliese 876 d, an exoplanet orbiting the nearby star Gliese 876, was the first exoplanetary system to feature a terrestrial planet, a major find in the search for exoplanets. Gliese 876 had been previously found to harbor two large gas giants in the aforementioned article by Geoff Marcy. Also of note, Gliese 876 is a red dwarf, a very low mass star that was previously thought to be incapable of harboring any significant planetary companions. This led further credence to the lessons learned from the discovery of PSR 1257+12 – that the conditions

---

<sup>3</sup> Mayor, M. & Queloz, D. A Jupiter-mass companion to a solar-type star. *Nature* 378, 355-359 (1995)

<sup>4</sup> Marcy, Geoffrey W. et al. Three New 51 Pegasi-Type Planets. *The Astrophysical Journal* 474 (1997).

necessary for the development of exoplanets were not as limited as previously thought. The key findings of the discovery of Gliese 876 d were highlighted in a 2005 paper published in the *Astrophysical Journal* by a team led by Eugenio Rivera of the Lick Observatory in California.<sup>5</sup>

In 2006, a team led by Paul Kalas, Professor of Astronomy at UC Berkeley, used the Hubble Space Telescope's new vortex coronagraph to examine the nearby star Fomalhaut, in the constellation of Pisces Austrinus. Upon observing the star, the team discovered within its diffuse dust cloud, an exoplanet lurking amongst the debris, this providing the first directly imaged exoplanet in history. His findings were published in *Science* in late 2008 titled "Optical Images of an Exosolar Planet 25 Light-Years from Earth".<sup>6</sup>

Perhaps the most astonishing exoplanetary discovery in recent memory has been the observation of an exoplanet orbiting our closest stellar neighbor, Alpha Centauri. Published by a team from the Geneva Observatory in 2008 (the same observatory which discovered the first main-sequence exoplanet, 51 Pegasi b), the planet Alpha Centauri Bb, a large terrestrial planet, is currently being investigated for confirmation by almost a dozen astrophysical research teams. The implications of the discovery of an Earthlike planet, only 4.3 light years away, could provide a strong future impetus for interstellar travel and exoplanetary colonization.<sup>7</sup>

---

<sup>5</sup> Rivera, Eugenio J. et al. "The Lick-Carnegie Exoplanet Survey: A Uranus-mass Fourth Planet for GJ 876" (2010).

<sup>6</sup> Kalas, Paul; et al. "Optical Images of an Exosolar Planet 25 Light-Years from Earth". *Science* 322. (2008)

<sup>7</sup> Dumusque et al. "An Earth mass planet orbiting Alpha Centauri B". *Nature* 490. (2012)

## 5. Technical Background

### 5.1 Principal Methods for the Detection of Exoplanets

Since the 1992 discovery of the PSR 1257+12 system, there have been over a dozen methods that have been developed for the reliable detection and confirmation of exoplanetary systems. However, of the various methods that have been used, there are two methods that have been found to be the most versatile in tackling the many problems presented by stellar systems that may be found throughout the universe. These two methods are known as the **radial velocity method** and the **transit method**. In the following sections, we shall give a brief overview of the theories behind them, as well as an example of their use and functionality as used in the detection of exoplanets.

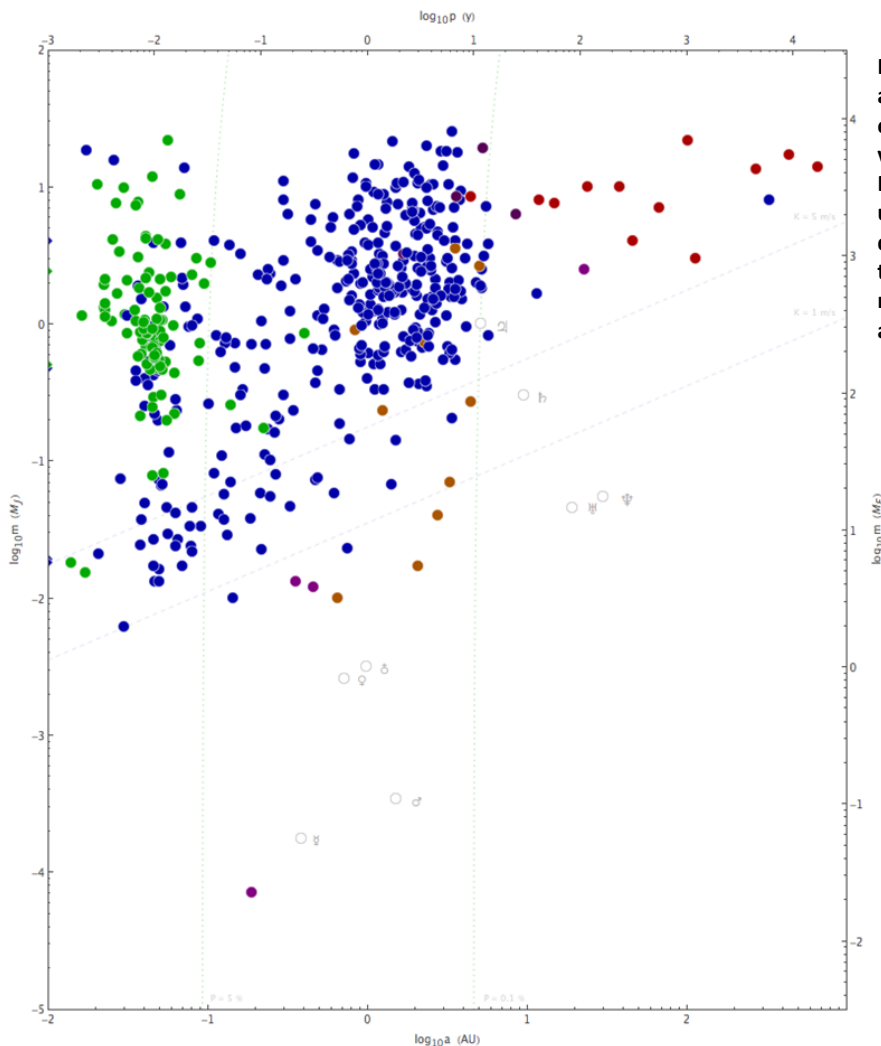


Figure 1: A plot of the orbital distance and size parameters for a selection of exoplanetary discoveries highlighting the various methods used in their detection. Blue dots represent discoveries made using the radial velocity technique, green dots represent discoveries made using the transit method. Note how the vast majority of discoveries made were achieved using these two methods.

### 5.1.1 The Radial Velocity Method

Accounting for about 70% of all known exoplanetary discoveries, the radial velocity method is generally seen by astronomers as the most reliable means of detecting exoplanets. In simple terms, the radial velocity method seeks to measure the degree to which an exoplanet gravitationally affects its parent star due to the motion of the planet along its orbital path.

This effect can be explained if one considers a gravitationally bound two-body system, encompassing a large star and a smaller planet. Stars are near-blackbodies which have a specific peak emission wavelength depending on the temperature of their photosphere, which is the source of a star's color (for more on Stellar Spectra and Classification, see Appendix \_\_) and this is used to our advantage in the Radial Velocity method's technique.

As we know from the two-body system, the orbital balance of the two objects will not be at the center of the larger mass, but at some location between the two objects, known as a barycenter. The distance of the barycenter from the center of the larger body is determined by the relative masses of the two objects. Both the star and the planet orbit around this center of mass. This will produce a noticeable “wobble” in the star's apparent position because it is, in fact, orbiting the barycenter just as the planet is. The diagram below visually illustrates this barycentric phenomenon, showing how the planet's motion affects the system.

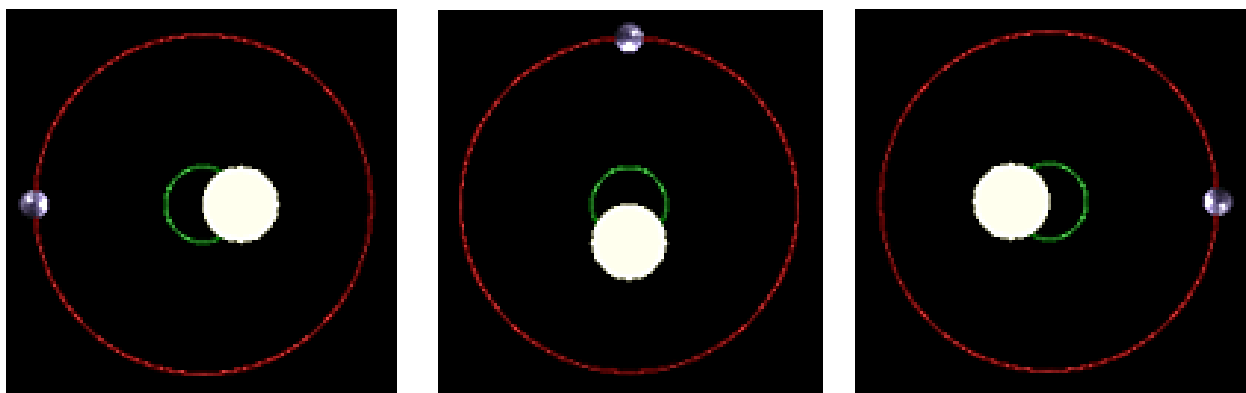
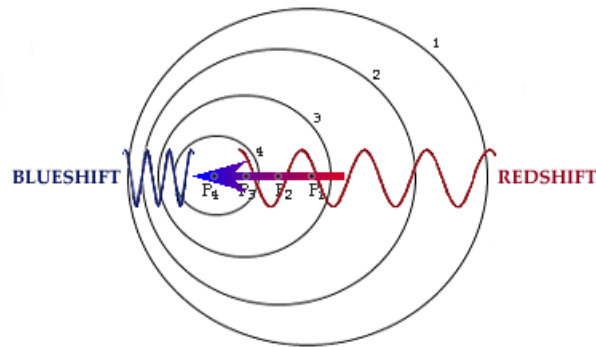


Figure 2: Simple graphic exhibiting the “wobbling” motion of a star around its barycenter due to the presence of a planet.

Now, because the stellar system is no longer “static”, the wobble of the star produces a slight change in the star’s normally static spectral output. As we recall from elementary physics, this result is known as the Doppler Effect, which (assuming that the star is moving only in the radial direction) can be expressed with the following formula:

$$1 + z_{radial} = \sqrt{\frac{1 + \frac{v}{c}}{1 - \frac{v}{c}}}$$

Where  $z_{radial}$  is the redshift of the system,  $v$  is the radial velocity, and  $c$  is the speed of light.



**Figure 4: A simple graphic illustrating the concept of wavefront compression and expansion as observed in the Doppler Effect and the subsequent visual effect that it has on wavelength.**

As the star orbits the barycenter, the light that it is transmitting is shifted based on its motion toward or away from the detection point (which in our case is Earth). When the star recedes away from us, the wavefronts of light are spaced further apart, shifting the emitted light towards the red end of the spectrum. When the star approaches us, the opposite effect occurs, the wavefronts are compacted together, yielding a shorter set of wavelengths, causing the light to shift towards the blue end of the spectrum. The graphic below illustrates the effect.

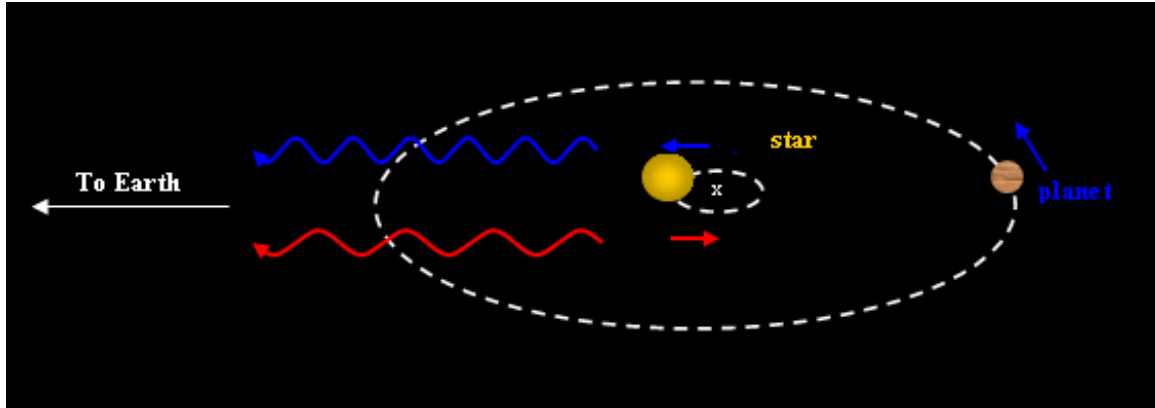


Figure 6: A diagram combining the two previous ideas to show the principles of the radial velocity method.

By measuring the extent to which the star is red or blueshifted, as well as the total period during which the shift occurs, astronomers can gather a great deal of information about the exoplanetary system, including the relative size of a planet in comparison to the star, its orbital period, and the planet's orbital distance and velocity. Assuming a circular orbit, the principal equation used in this calculation is:

$$r^3 = \frac{GM_{star}}{4\pi^2} P_{star}^3$$

Where  $r$  is the orbital radius of the planet,  $G$  is the Gravitation Constant of the Universe,  $M_{star}$  is the mass of the parent star, and  $P_{star}$  is the parent star's oscillation period. Knowing any two of the variables allows us to find the third – in most cases, we know the mass of the star, and, obviously, the oscillation period, which then tells us the orbital radius of the planet.

If we expand the system to the more accurate and useful elliptical models, we attain the generalized, but more cumbersome formula:

$$V_r = K [\cos(\omega + \theta) + e \cos \theta], \quad K \equiv \frac{2\pi}{P} \frac{a_* \sin i}{(1 - e^2)^{1/2}}$$

Where  $V_r$  is the radial velocity,  $K$  is the semi-amplitude of the radial velocity curve,  $\omega$  is the argument of the periapsis,  $\theta$  is the true anomaly,  $e$  is the eccentricity,  $i$  is the inclination of the planet's orbit,  $a$  is the semimajor axis of the orbit, and  $P$  is the orbital period.

However, while the radial velocity technique is useful in a wide variety of cases, it is not always of benefit to use. One of the major difficulties that befalls the radial velocity method is that it has difficulty detecting planets that are so small as to become insignificant compared to the mass of their parent star. In this case, the difference in mass between the star and the planet is so great that the gravitational effect of the planet on the star is almost negligible, producing very little wobble, and therefore, very little change in perceived spectral output. In some cases, the oscillatory motion may be so minute that the signal will be drowned out by background noise, and spectrographs will not be able to detect the movements at all.

Another limitation of this method is that if the orbit of the planet is perpendicular to the line of sight of the observer, the planet will not be detected because there will be no axial shift in the star's position, and therefore, there will be no spectral shifting.

And finally, due to signal-to-noise limitations, this method is generally not effective for stars lying further than 200 light years, but with improvements in the sensitivity of spectrographs, this number is generally increasing each and every year.

### **5.1.2 The Transit Method**

The transit method, another widely used method in the field of exoplanetary study, accounting for around 20% of all exoplanetary discoveries, will receive special attention in this paper. Although it is perhaps not as versatile as the radial velocity method, it is still a popular and convenient means for discovering exoplanets.

The transit method is a convenient method because of its relative simplicity - one does not need a complex and finely-tuned spectrograph in order to make measurements with this method. Making use of a photometer and widely available digital analyzing equipment, the transit method is a widely accessible means of detecting and discovering exoplanets.

The transit method takes advantage of the convenient positioning of a planet as it crosses the disc or corona of its host star. When this occurs, astronomers are able to measure a slight, but noticeable drop in the photometric reading of the star, which then can be analyzed to provide a

variety of useful information regarding the exoplanetary system. The graphic below provides a nice introduction to the basic idea behind the method:

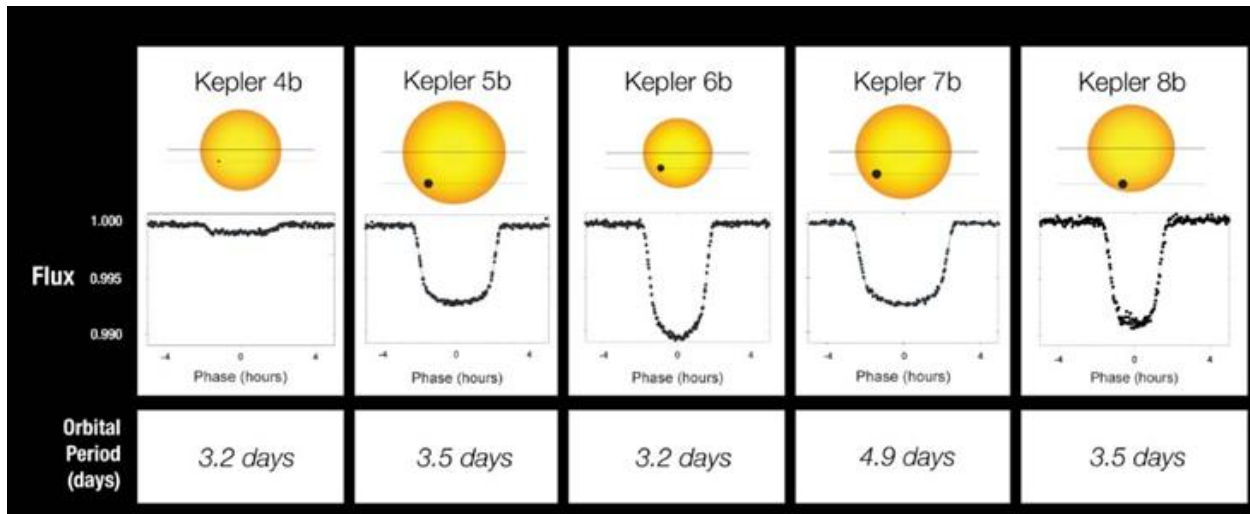


**Figure 8:** A diagram displaying the photometric light curves gathered from a number of different planets from the Kepler Exoplanetary Survey mission. Note, the ratios of the planets to the stars and the maximum depth of the light curve.

As we observe, there are several parameters that must be taken into account when using the transit method to study exoplanetary systems: the cross-sectional disc of the planet relative to its host star, the azimuthal location along the disc of the star, and the transit period from ingress to egress. These may all be gathered from the light curve profile shown above.

As an exercise, let us define the steps of analysis for a given light curve profile, to demonstrate how astronomers gather information from these seemingly simple, but very revealing datasets.

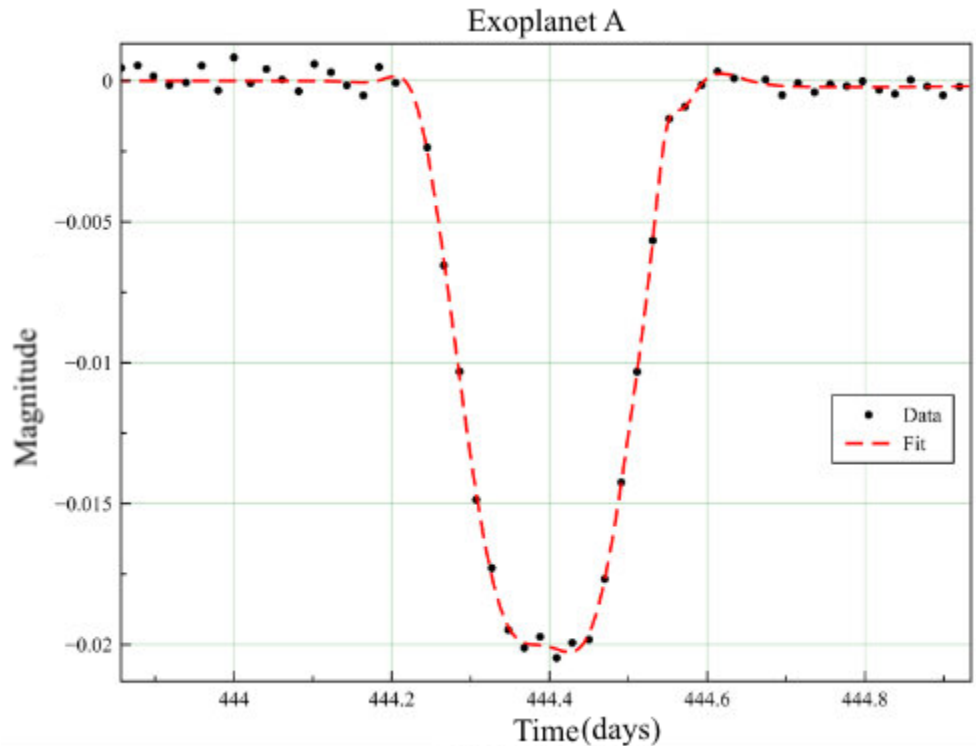


**Figure 9: A sample light curve gathered for the hypothetical “Exoplanet A”**

Taken from the sample photometric measurement for Exoplanet A above, we find that the width of the light curve of the parent star (which corresponds to the total transit time of the planetary system) is found to be approximately 0.4 of a day. The maximum dip of the light curve (which corresponds to the effect of the exoplanet crossing the disc of its star) is found to be about 0.2 of a magnitude. We also find from observing the ingress and egress periods (that is, the point where the planet just crosses over into the disc of the star), that the time that the planet takes to cross into the disc is approximately 75% of a half period, or about 0.15 days. From this information, we can learn a surprising amount of detail about Exoplanet A.

First, from the total transit time, it is possible to calculate the period of the transit, which can then tell us the average velocity of the planet’s motion in the region where the planet crosses that star’s disc. As we are observing from a great distance, we can essentially reduce a transit event to a one-dimensional problem of motion – that of a 1D oscillator and can reduce the three-dimensional celestial bodies into two-dimensional cross-sections. In simple, everyday terms, one

can think of a small, dark circular piece of paper sliding over the top of a large, bright circular piece of paper.

From this simple visual model, one can indeed find the ratio of the planet's cross-sectional area to that of its parent star by simply making use of the given formula:

$$\frac{A_p}{A_s} = \frac{\pi r_p^2}{\pi r_s^2}$$

Where A is the cross-sectional area of the planet/star respectively and r is the radius.

Furthermore, if one knows the radius of the star (which is generally calculable using the Mass-Radius relationship based on the famous Mass-Luminosity relation, one can gain a reasonable estimate for the radius of the planet.

Since the size of the host star is known, and the vantage point at which we are observing the system is well beyond the range where any kind of angular difference would throw off the measurement, attaining an estimate of the planet's 2-D cross section is not generally a difficult task. Depending on the size of the planet, and from information gleaned from atmospheric scattering effects that might be observed during the ingress and egress periods of the transit, one might also be able to make a ballpark estimate of the planet's mass by using an assumed density based on the relative size of the planet to its host star.

For a terrestrial planet, assuming a molten core, large mantle, and relatively thin crust, like that found in our Solar System, a reasonable estimate for the average density would be  $4.5 - 5.0 \frac{g}{cm^3}$ .

For a gas giant, assuming that it is similar to the gas giants found in our Solar System, a typical average density estimate would be about  $0.7 - 1.4 \frac{g}{cm^3}$ .

From our knowledge of planetary hydrostatic equilibrium, we know that planetisimals larger than about 500 kilometers are generally spherical in shape. Because exoplanets of that size are too small to be currently detected by our instruments, we can assume that all exoplanets that have been currently discovered are near-spherical in shape. This makes our calculations easy.

Assuming a spherical planet and uniform density, a simple estimate of the mass of an exoplanet can be found by using the following formula:

$$M_p = \left(\frac{4}{3}\pi r_p^3\right) * \rho$$

Where  $r_p$  is the radius of the planet, and  $\rho$  is the average density of the planet.

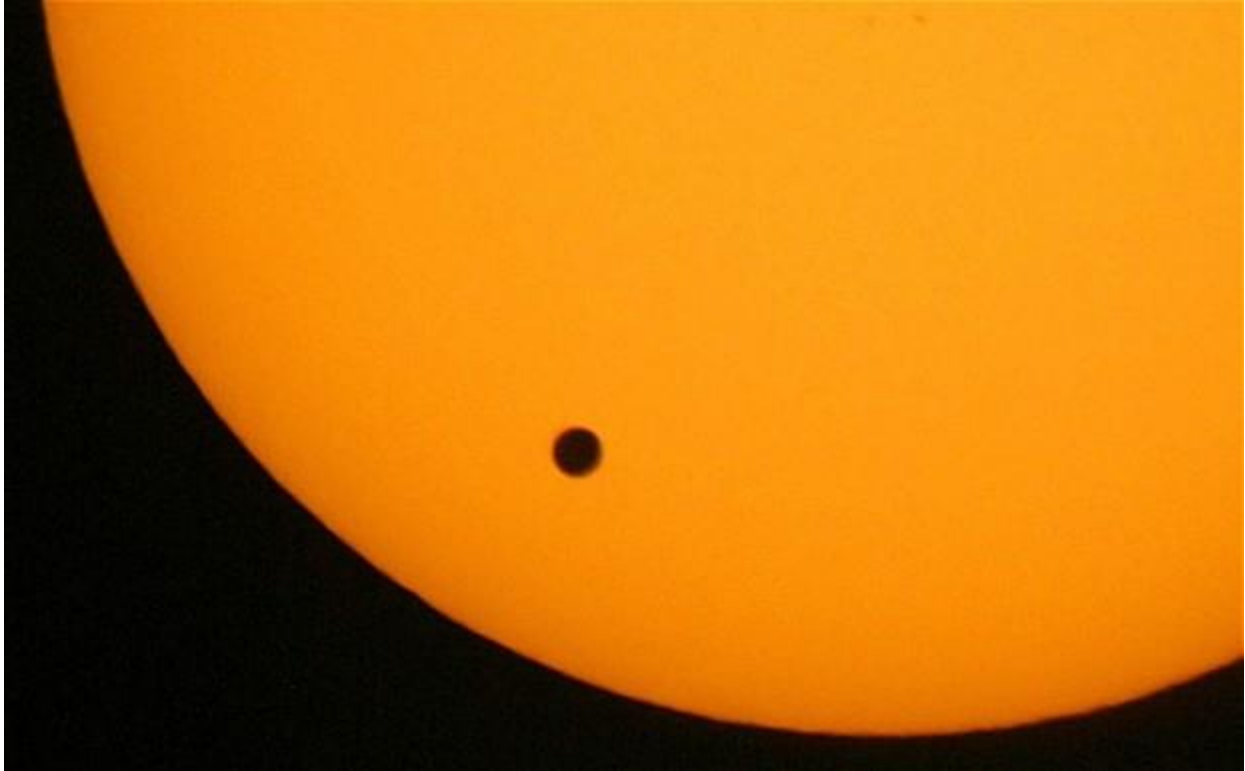


**Figure 10: Venus transiting the Sun. Note how dark the disc of the planet is in comparison to the Sun's emitting surface. One can see, however, the effect that the atmosphere has – the thick, diffuse atmosphere scatters and reflects.**

The transit time, otherwise known as  $t_{transit}$  can be found for any elevation that the planet crosses the star's disc if we assume a near-circular orbit (this is not *always* the case, but it turns out to be a generally reasonable assumption). We begin by first calculating the length of the planet's path across the disc. This can be expressed as:

$$l = \sqrt{(R_s + R_p)^2 - b^2}$$

Where  $l$  is the half length of the transit,  $R_s$  and  $R_p$  are the radii of the planet/star, respectfully, and  $b$  is the so-called “impact parameter” based on the inclination of the planet and the orbital distance. It is defined as:

$$b = a \cos i / R_s$$

Where  $a$  is the orbital distance of the planet during the transit. We note especially from this expression that if  $b = 0$ , that is, if the planet crosses the disc of the star at its widest point, it eliminates the term from our previous expression.

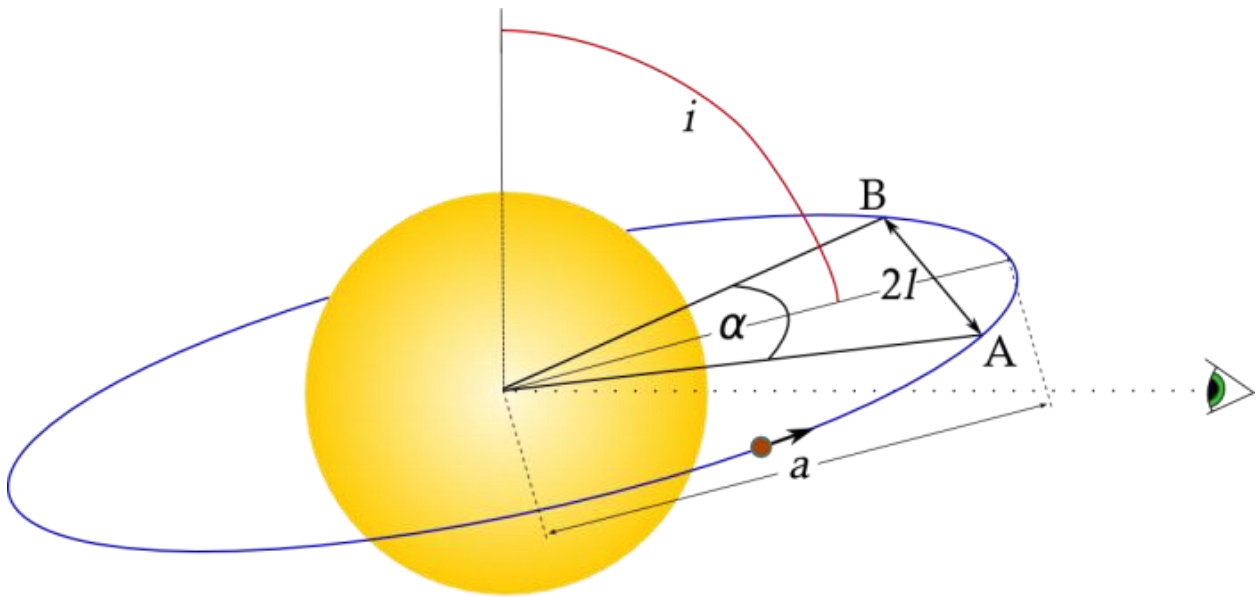


**Figure 11: Graphic explaining the various parameters in the derivation of transit time problem.**

As observed in the above graphic, the triangle made from point A (the ingress), point B (the egress), and the center of the star, sweeps out an area that we shall call angle  $\alpha$ . Angle  $\alpha$  is the angular distance that a planet travels during its transit. Knowing this, we observe that the sine of angle  $\alpha$ , will be equal to the total length of the transit, or  $2l$ . Therefore, we can say that:

$$\sin(l) = \sin\left(\frac{\alpha}{2}\right)$$

From the geometry of the graphic, we also see that  $\sin\left(\frac{\alpha}{2}\right)$  can also be expressed as  $\frac{l}{a}$ .

Since a total orbit of the planet around the star would be  $2\pi a$ , then the distance travelled during the transit would be simply  $\frac{\alpha a}{2\pi a} = \frac{\alpha}{2\pi}$ . Now, knowing this, if we know the period of the planet's orbit  $P$ , then we can solve for the transit time by simply multiplying  $P$  by the angular fraction and then plugging in previously-found expressions.

$$t_{transit} = \frac{P\alpha}{2\pi} = \frac{P}{\pi} \sin^{-1}\left(\frac{l}{a}\right) = \frac{P}{\pi} \sin^{-1}\left(\frac{\sqrt{(R_s + R_p)^2 - b^2}}{a}\right)$$

The period of time between transit events as observed on light curves will also tell us the total orbital period of the exoplanet, since that is the total time that it takes for the planet to return to its original position. However this can sometimes be a bane to astronomers, since from the observation of only a single transit event, one cannot always be certain when the next event will occur in any reasonable amount of time, and it is always a possibility that the planet will have an eccentric orbit and will take a very long time to return to the “transit zone”. As we know from Kepler’s Laws of Planetary Motion, planets that travel around a star “sweep out equal areas in equal times”, meaning that a planet with a highly elliptical orbit travelling near to its *periastron*<sup>8</sup>

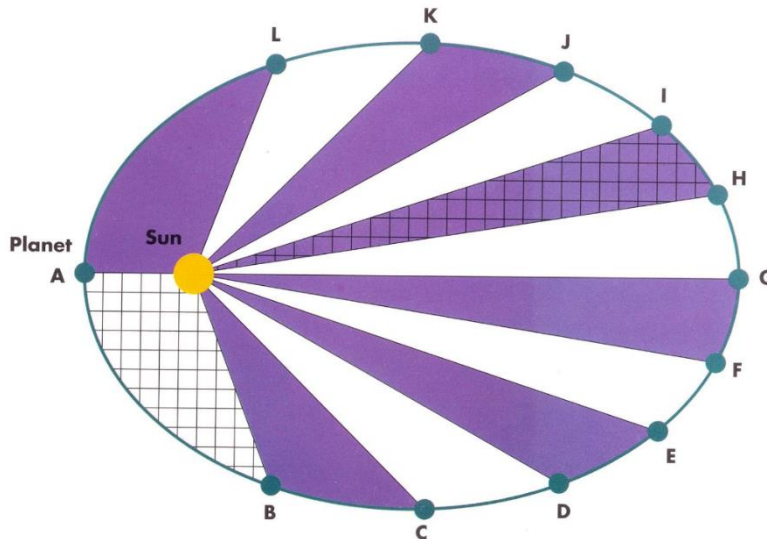
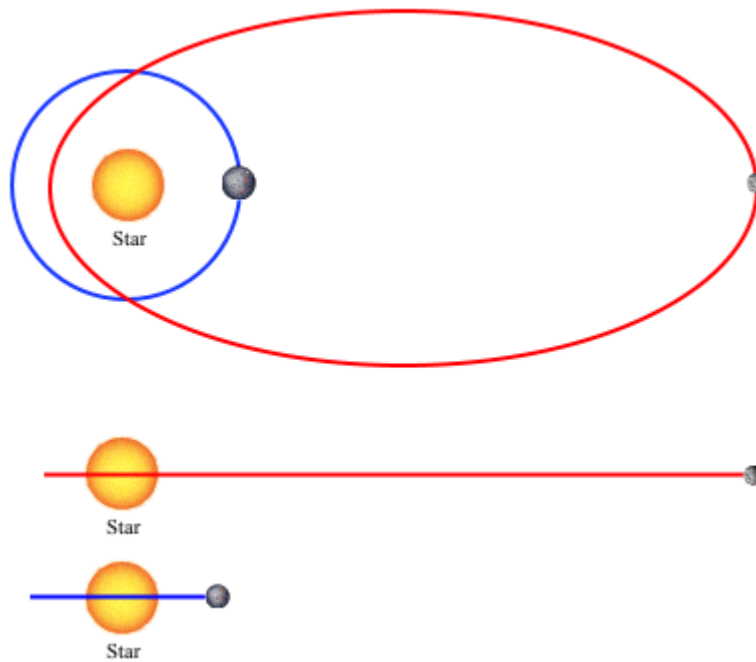


Figure 12: Kepler’s principle of “Sweeping out equal areas in equal times”

<sup>8</sup> From Greek  $\pi\epsilon\rho\acute{\iota}$  = “around” and  $\acute{\alpha}\sigma\tau\rho\omicron\nu$  = “star”. In other words, the orbital point closest to the star.

will advance much further along its orbital path than when it is at its *apoastron*<sup>9</sup>. The graphic below illustrates this point.

As we observe, the time that the planet takes to cross the disc of the star can be exceptionally small compared to the time that is taken to complete the rest of its orbit, thus playing into the potential for long gaps between transit events. This is why it is extremely important to record transit events as they occur, for they may never come again in a lifetime.



**Figure 13: A simple comparison of planets with circular and highly eccentric orbits. Planets with high eccentricities may be misleading because their orbital velocities will be high for a short time while they are near their parent star, but very slow elsewhere.**

One may also determine the ratio of the diameter of the planet to its parent star by using the maximum drop in magnitude on the light curve as a gauge for the percentage of light lost when the planet blocks out the disc of the star as it passes in front of it. As we know, stars produce light, while planets either reflect or absorb the light produced by the stars. When viewed from afar, planets crossing in front of the stellar disc block the light emitted from their parent star.

---

<sup>9</sup> The opposite of the periastron. From Greek *απο* = "from" and *ἄστρον* = "star".

In highly sensitive transit method measurements, astronomers will also take into account detailed models that measure and analyze minute photon scattering effects caused in three-dimensions that occur on the ingress and egress period of the transit event. In this manner, astronomers can gain a surprisingly detailed understanding of the composition of the planetary atmosphere, but this is a whole topic unto itself.

The effects of limb darkening are also compensated for in the most detailed models. Although for our purposes, it will not be a considered factor, many studies have been conducted on this peculiar and complicated phenomenon. Limb darkening occurs in stars due to a radial drop in density as one moves outward from the core. As the material of the star becomes less dense, it cools, leading to edges are dimmer than the star's center. Because of this, transit measurements may be thrown off slightly because of the effect of the photometer picking up darkening edges (especially during the ingress and egress periods) than the star may actually be emitting.

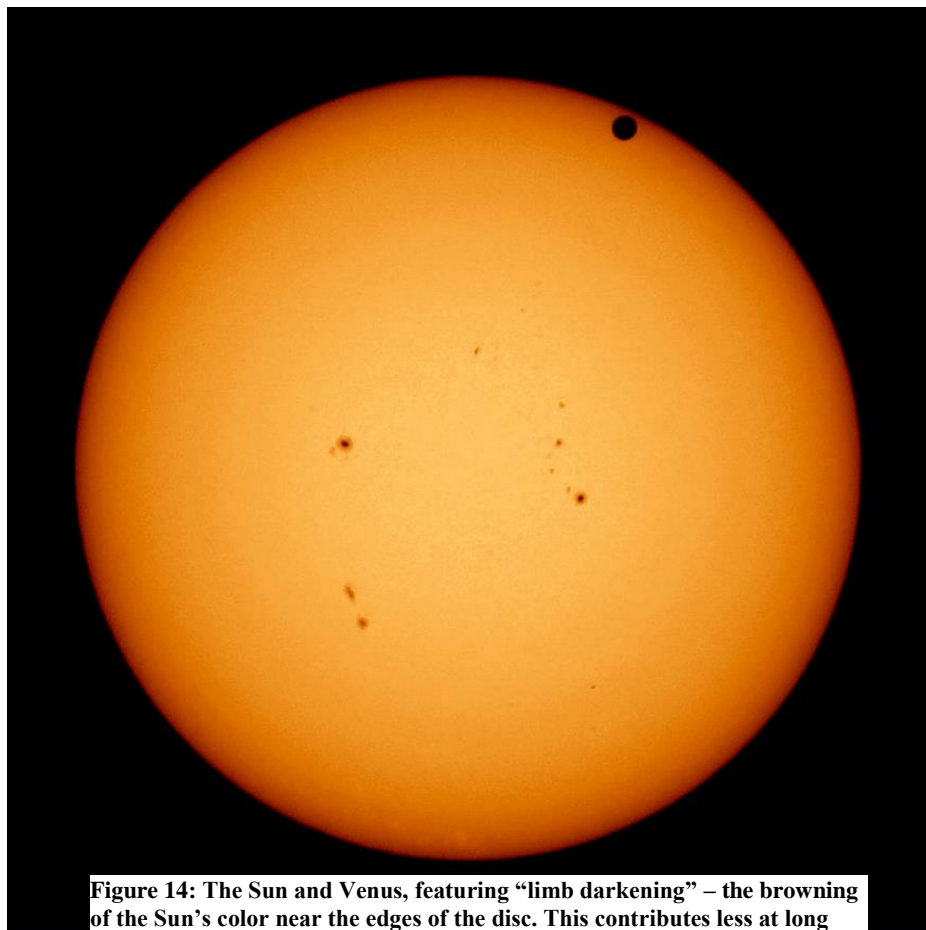


**Figure 14: The Sun and Venus, featuring “limb darkening” – the browning of the Sun’s color near the edges of the disc. This contributes less at long distances, but still requires correction algorithms in sensitive analyses.**

## 5.2 Other Methods for the Detection of Exoplanets

Despite composing only about 10% of all exoplanetary finds, there are a number of other exoplanetary detection methods that have been used by astronomers over the years. Generally, these methods are useful in only very specific situations, which means that many astronomers prefer to use either the transit method, or the radial velocity method in most cases. I shall briefly touch upon each of the methods below.

### 5.2.1 The Pulsar Timing Method

The pulsar timing method is the oldest method that has been used successfully to detect exoplanets, since it was the method that detected the planets orbiting PSR 1257+12 in 1992. The pulsar timing method takes advantage of the fact that pulsars output a highly focused burst of electromagnetic radiation at precise intervals. These pulsar bursts emit regularly for millions of

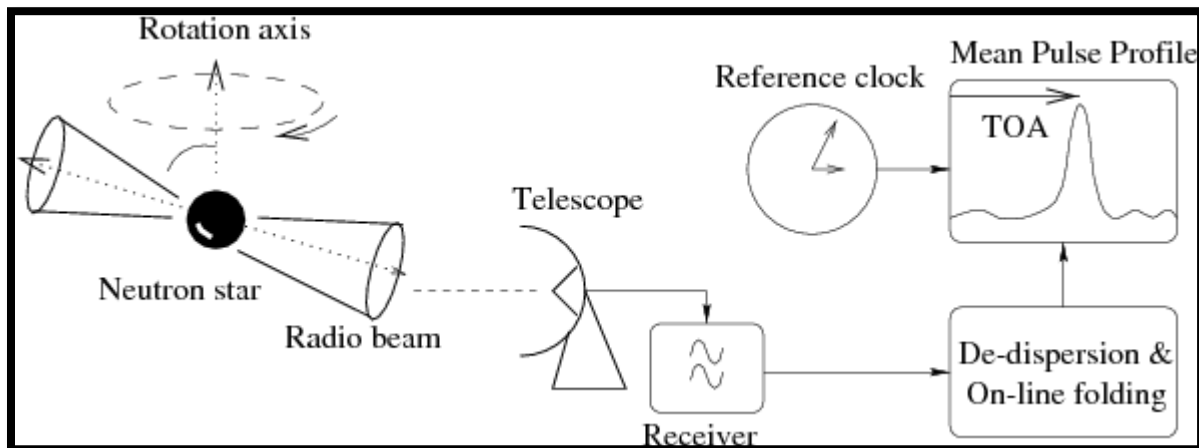
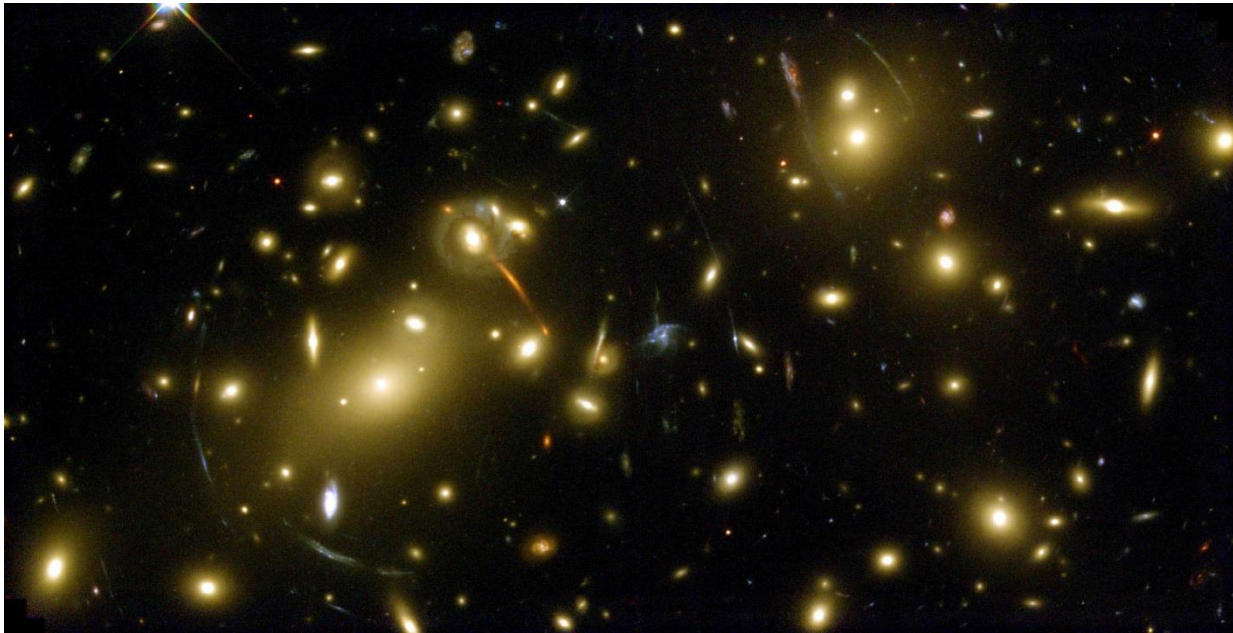


Figure 15: A diagram exhibiting the basic process of the Pulsar timing method.

years before the timings become less regular and the signals start to degrade significantly due to a gradual loss of the pulsar's angular momentum over time. Analyses of pulsar emission curves allow astronomers to detect minute, unexpected irregularities in the timing of a pulsar's pulses (they establish an age depending on the regularity of the pulsar), which in turn allows them to utilize computer-aided curve fitting and planetary modelling to find out the root cause of the irregularity.

The benefit of the pulsar timing method is that it is extremely accurate due to the regularity of the pulsar timings. However, the downside is that the requirements for this method are extremely specific: it requires pulsars, which are quite rare, and generally very distant, to work.

### 5.2.2 The Gravitational Lensing Method



**Figure 16: One of the most famous images featuring gravitational lensing – galaxy cluster Abell 2218. Note the “fisheye effect” near the center of the image caused by the extreme combined mass of several large galaxies in the foreground.**

The gravitational lensing method is a rare method that has only been used on a handful of occasions since it requires a very chance lineup of events in order to be used. When a massive object passes very near to a distant object located behind it, the gravitational lensing caused by the object in the foreground “magnifies” the image of the object behind it. One event of interest was the gravitational lensing of the star OGLE-2005-BLG-390L, an exoplanetary system located a staggering 21,500 ly + 3,500 ly away. Under normal circumstances, a planet at this distance would not even have a remote chance of being detected, but due to the gravitational microlensing caused by the passing of a nearby star, astronomers were able to observe this once-in-a-lifetime a transit event of the exoplanet in orbit around the aforementioned star. Due to the sheer luck involved in identifying the microlensing event, and the vast distance involved, this particular exoplanetary system may never be observed again. This is why it is important to observe microlensing events as they occur, since they are only likely to occur once.

### 5.2.3 The Direct Observation Method

Up until very recently, exoplanets could only be observed through indirect methods (either counting photons, as in the transit method, or observing spectral signatures, as with the radial velocity method). But in 2007, the invention of the vortex coronagraph changed all that. Vortex coronagraphs operate in a similar manner to traditional coronagraphs in that they block out the most of the blinding light produced by a star and allow astronomers the ability to observe solar prominences and other phenomena occurring in a star's corona. However, previously, these coronagraphs were only used to observe our Sun. With some significant modifications, the vortex coronagraph allows astronomers to train the vortex coronagraph on other stars, and allowing them to directly observe the dim glow of extrasolar planets.

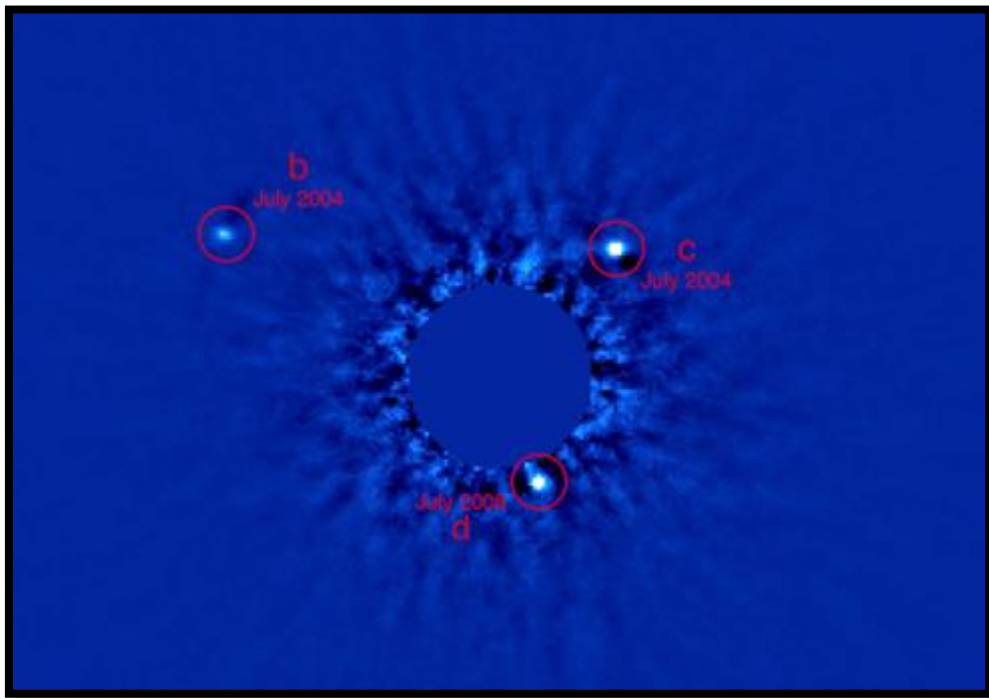


Figure 17: Exoplanets around Fomalhaut directly imaged using a vortex coronagraph. Note the mask used to block out the blinding rays of the star to allow the planets to be observed.

The benefits of direct observation are that it allows astronomers to directly image exoplanets and observe things such as albedo, diffusivity, size, orbit, and many other properties. The only significant downsides to direct imaging is that vortex coronagraphs are new technology and are therefore prohibitively expensive. Additionally, vortex coronagraphs are only as good as the

telescope they are attached to, so they may have a limited viewing range if not integrated for use with the largest of space telescopes.

#### 5.2.4 The Astrometric Method

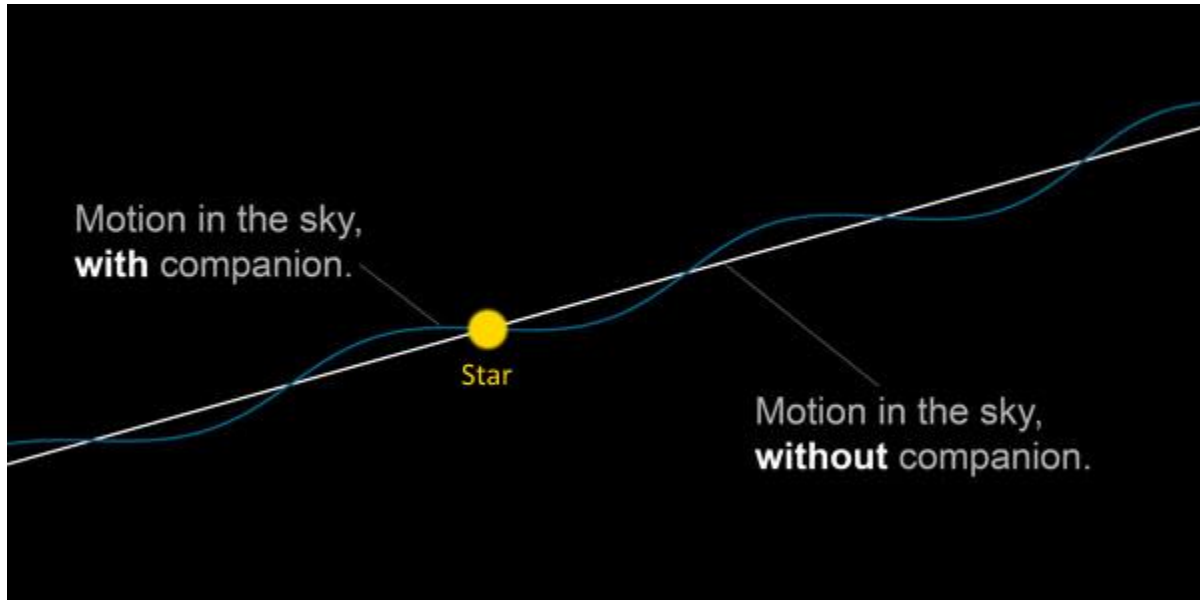


Figure 18: A simple illustration showing the basic idea behind astrometry.

The astrometric method is a very old method that dates back many centuries. It makes use of the positions of stars as they move through space to determine if there are unseen companions that may be affecting the barycenter of the star system. This is the method that Herschel used in his report of the “third companion” of 70 Ophiuchi, as well as the rumors of the planet orbiting Barnard’s star in the 1950s.

Although astrometry is a simple method, it has a number of very significant downsides, including the fact that it has historically produced many false positives, therefore being generally unreliable without all but the best equipment, and that it can only be used assuming that the star’s parallax is significant enough to be measured. Due to these limitations, only a handful of exoplanets have been discovered and confirmed using this method.

## 6. Statistics of Current Exoplanet Discoveries

### 6.1 Goals

The goal of the second stage of the project was to gain an overarching understanding of the general trends that can be found with the current number of potential exoplanetary systems. Using a combined set of databases gathered from the various exoplanet surveys, we hoped to gain a more complete understanding of the types of stars that these exoplanets form around, as well as their locations in the local region of space. Using this information, we wanted to construct the image of the “ideal star”, that is, the star that was most likely to harbor transiting exoplanets, which would play into the third stage of the project.

### 6.2 Sources

The sources used for the statistical overview of current exoplanetary findings are diverse, a large aggregate of data gathered from NASA’s Exoplanet Archive, including data from the SIMBAD, VizieR, Kepler Mission, CoRoT, TrES, OGLE, and SuperWASP missions. Below, I shall give a short overview of the objectives set forth by these exoplanetary archives and missions.

NASA Exoplanetary Archive – An all-encompassing archive developed by NASA that seeks to provide information from all exoplanetary databases in one easy to use location. The data used in this report was gathered primarily through the online resources stored within this archive.

SIMBAD – Standing for “**S**et of **I**dentifications, **M**easurements, and **B**ibliography for **A**stronomical **D**ata”, SIMBAD is hosted by the Strasbourg Astronomical Data Center in Strasbourg, France and provides to astronomers data on over five million astronomical objects.

ViZieR – The VizieR database, also hosted by the Strasbourg Astronomical Data Center in Strasbourg, France is another database which supplies data primarily found in journal publications. It contains nearly 10,000 catalogues of information on various topics within the realms of astronomy and astrophysics.

Kepler – Named for the famous astronomer Johannes Kepler, the Kepler mission was launched in 2009 as an automated transiting exoplanet search able to identify exoplanetary systems in a region of the galaxy between Cygnus and Lyra. Although the mission was discontinued in 2013 due to mechanical problems with the Kepler orbiter, throughout the duration of the mission, Kepler succeeded in identifying nearly 4,000 potential exoplanetary systems, of which nearly a quarter were confirmed.

CORoT – Standing for “**C**Onvection **R**Otation and planetary **T**ransits”, the CORoT mission, launched by the French Space Agency, ran from 2007 until its demise in 2013 due to mechanical problems. The mission’s goal was to examine transiting exoplanets, particularly those with short periods in the hopes of finding a terrestrial-type planet.

TrES – The “**T**rans-atlantic **E**xoplanet **S**urvey” was a smaller exoplanetary survey consisting of a network of small telescopes to identify exoplanets. It was able to detect and confirm five separate exoplanetary systems throughout its short duration.

OGLE – The Optical Gravitational Lensing Experiment is a long-lived project begun by Poland’s University of Warsaw consisting of three separate searches (OGLE I-III) which have succeeded in detecting exoplanets using the rare gravitational lensing method described in previous sections. About 20 exoplanets have been confirmed so far in the three searches.

SuperWASP – Super (**W**ide **A**ngle **S**earch for exo**P**lanets) is arguably one of the most extensive and ambitious exoplanetary searches still in operation today. Consisting of many multinational teams based in approximately twenty academic institutions all over the world, this mission seeks to scan the entire sky for transiting exoplanetary systems. The exoplanet that was observed in this report was selected from the one hundred plus exoplanets discovered in the WASP mission.

## 6.3 Data Analysis

### 6.3.1 Exoplanetary System Characteristics

| Planet Name |                      | A      | B       | C      | D          | E     | F     | G        | H   | I          | J            | K         | L                  | M       | N       | O      | P    | Q     | R     | S         | T         | U         | V         | W    | X | Y | Z |  |  |
|-------------|----------------------|--------|---------|--------|------------|-------|-------|----------|-----|------------|--------------|-----------|--------------------|---------|---------|--------|------|-------|-------|-----------|-----------|-----------|-----------|------|---|---|---|--|--|
| 34          | HAT-P-6 b Transit    | 3.853  | 0.05237 | 0      | 2.016+27   | 1.059 | 1.33  | 0.132338 | Yes | 2.370E+10  | -3.9005E-11  | 0.9482329 | 85.51              | 354.774 | 42.466  | 6370   | 1.46 | F2-F3 | F3    | 1.372E+27 | 3.527     | 2.727E+30 | 1.37      |      |   |   |   |  |  |
| 35          | WASP-24 b Transit    | 2.341  | 0.08851 | 0      | 2.0328E+27 | 1.071 | 1.3   | 0.129353 | Yes | 1.8868E+10 | -1.4934E-11  | 0.2818075 | 83.64              | 227.216 | 2.343   | 6075   | 1.33 | F0-F1 | F0    | 1.294E+27 | 3.326     | 2.407E+30 | 1.21      |      |   |   |   |  |  |
| 36          | CoRoT-19 b Transit   | 3.897  | 0.0518  | 0.047  | 2.1068E+27 | 1.11  | 1.29  | 0.128358 | Yes | 2.7462E+10 | -4.51428E-11 | 1.2397176 | 88                 | 97.034  | -0.171  | 6090   | 1.65 | F0-F1 | F0    | 1.294E+27 | 3.326     | 2.687E+30 | 1.35      |      |   |   |   |  |  |
| 37          | OGLE-TR-11 b Transit | 1.690  | 0.0035  |        | 2.2396E+27 | 1.18  | 1.2   | 0.119403 | Yes | 1.6259E+10 | -8.7166E-12  | 0.0792099 | 83.4               | 162.645 | -61.957 | 6210   | 1.32 | F0-F1 | F1    | 8.952E+26 | 2.301     | 2.451E+30 | 1.23      |      |   |   |   |  |  |
| 38          | OGLE-TR-4 b Transit  | 1.212  | 0.01942 | 0      | 2.6382E+27 | 1.39  | 1.378 | 0.137114 | Yes | 1.8776E+10 | -2.20295E-12 | 0.0413619 | 73.72              | 269.148 | -29.539 | 6050   | 1.36 | F0-F1 | F0    | 8.506E+26 | 2.201     | 2.424E+30 | 1.22      |      |   |   |   |  |  |
| 39          | WASP-12 b Transit    | 1.091  | 0.0229  | 0.089  | 2.6782E+27 | 1.41  | 1.79  | 0.176109 | Yes | 1.8554E+10 | 3.1820E-12   | 0.0526738 | 83.1               | 97.837  | 29.872  | 6300   | 1.57 | F0-F1 | F1    | 1.341E+27 | 3.448     | 2.712E+30 | 1.36      |      |   |   |   |  |  |
| 40          | HAT-P-8 b Transit    | 3.076  | 0.0487  | 0      | 2.888E+27  | 1.52  | 1.5   | 0.149254 | Yes | 2.208E+10  | 3.96485E-11  | 0.8754545 | 87.5               | 343.041 | 35.447  | 6200   | 1.58 | F0-F1 | F1    | 1.274E+27 | 3.276     | 2.677E+30 | 1.35      |      |   |   |   |  |  |
| 41          | HIP 29301 b Transit  | 4.114  | 0.05496 | 0      | 2.888E+27  | 1.522 | 1.286 | 0.127996 | Yes | 2.8647E+10 | 3.67892E-11  | 1.0538943 | 88.6               | 92.664  | 30.957  | 6210   | 1.73 | F0-F1 | F1    | 1.538E+27 | 3.953     | 2.806E+30 | 1.41      |      |   |   |   |  |  |
| 42          | XO-4 b Transit       | 4.125  | 0.0555  | 0      | 3.2646E+27 | 1.72  | 1.34  | 0.133333 | Yes | 2.565E+10  | 3.79603E-11  | 0.9736922 | 88.7               | 110.388 | 58.268  | 6397   | 1.56 | F2-F3 | F2    | 1.408E+27 | 3.619     | 2.745E+30 | 1.38      |      |   |   |   |  |  |
| 43          | WASP-3 b Transit     | 1.847  | 0.03151 | 0      | 3.3405E+27 | 1.76  | 1.29  | 0.128358 | Yes | 1.6986E+10 | -3.44113E-11 | 0.5845059 | 84.93              | 278.032 | 35.662  | 6400   | 1.31 | F2-F3 | F2    | 9.946E+26 | 2.557     | 2.516E+30 | 1.26      |      |   |   |   |  |  |
| 44          | Kepler-2 b Transit   | 2.205  | 0.032   | 0.039  | 3.3708E+27 | 1.776 | 1.363 | 0.135622 | Yes | 2.8045E+10 | 1.59105E-11  | 0.4463821 | 80.8               | 292.247 | 47.970  | 6350   | 1.84 | F2-F3 | F2    | 1.902E+27 | 4.888     | 2.959E+30 | 1.49      |      |   |   |   |  |  |
| 45          | WASP-61 b Transit    | 3.856  | 0.0514  | 0.26   | 3.9099E+27 | 2.06  | 1.24  | 0.123383 | Yes | 2.257E+10  | 1.00219E-11  | 0.2262419 | 89.25              | 75.300  | -26.054 | 6320   | 1.36 | F2-F3 | F2    | 1.019E+27 | 2.620     | 2.531E+30 | 1.27      |      |   |   |   |  |  |
| 46          | Kepler-5 c Transit   | 3.548  | 0.05064 | 0.024  | 4.0124E+27 | 2.114 | 1.431 | 0.142388 | Yes | 2.7748E+10 | -3.81232E-12 | 0.1057905 | 86.3               | 299.407 | 44.035  | 6297   | 1.79 | F0-F1 | F1    | 1.740E+27 | 4.474     | 2.854E+30 | 1.45      |      |   |   |   |  |  |
| 47          | HAT-P-31 b Transit   | 5.005  | 0.055   | 0.245  | 4.1306E+27 | 2.171 | 1.07  | 0.106468 | Yes | 2.7381E+10 | -3.7615E-11  | 1.0335548 | 87.1               | 271.538 | 26.427  | 6065   | 1.36 | F0-F1 | F0    | 8.645E+26 | 2.222     | 2.430E+30 | 1.22      |      |   |   |   |  |  |
| 48          | Kepler-40 b Transit  | 6.873  | 0.08    | 0      | 4.1756E+27 | 2.2   | 1.17  | 0.116418 | Yes | 4.0486E+10 | -8.5558E-12  | 0.3585246 | 89.7               | 296.814 | 47.527  | 6510   | 2.13 | F2-F3 | F3    | 2.815E+27 | 7.236     | 2.264E+30 | 1.64      |      |   |   |   |  |  |
| 49          | HAT-P-14 b Transit   | 4.628  | 0.0606  | 0.107  | 4.2363E+27 | 2.232 | 1.15  | 0.114428 | Yes | 2.4834E+10 | -1.45482E-11 | 0.3612857 | 83.5               | 260.116 | 38.242  | 6600   | 1.47 | F2-F3 | F3    | 1.416E+27 | 3.641     | 2.746E+30 | 1.38      |      |   |   |   |  |  |
| 50          | WASP-46 b Transit    | 4.086  | 0.0546  | 0.11   | 4.4034E+27 | 2.32  | 1.39  | 0.130308 | Yes | 2.8972E+10 | -2.1277E-11  | 0.6166446 | 85.9               | 156.225 | -34.990 | 6560   | 1.75 | F2-F3 | F3    | 1.983E+27 | 5.096     | 2.990E+30 | 1.50      |      |   |   |   |  |  |
| 51          | CoRoT-11 b Transit   | 2.994  | 0.0436  | 0      | 4.4223E+27 | 2.33  | 1.43  | 0.142289 | Yes | 2.0815E+10 | 3.76003E-12  | 0.0782617 | 83.17              | 280.687 | 5.938   | 6440   | 1.37 | F2-F3 | F2    | 1.115E+27 | 2.867     | 2.589E+30 | 1.30      |      |   |   |   |  |  |
| 52          | WASP-38 b Transit    | 6.872  | 0.07522 | 0.0314 | 5.1075E+27 | 2.691 | 1.094 | 0.108856 | Yes | 2.688E+10  | 6.00881E-11  | 1.6365641 | 88.69              | 243.960 | 10.033  | 6150   | 1.33 | F0-F1 | F0    | 8.742E+26 | 2.247     | 2.436E+30 | 1.22      |      |   |   |   |  |  |
| 53          | CoRoT-6 b Transit    | 8.887  | 0.0855  | 0.1    | 5.6181E+27 | 2.96  | 1.166 | 0.116602 | Yes | 2.3453E+10 | 5.41261E-11  | 1.2694368 | 89.07              | 281.073 | 6.663   | 6090   | 1.02 | F0-F1 | F0    | 4.944E+26 | 1.271     | 2.113E+30 | 1.06      |      |   |   |   |  |  |
| 54          | Kepler-43 b Transit  | 3.024  | 0.0449  | 0.025  | 6.1305E+27 | 3.23  | 1.2   | 0.119403 | Yes | 2.1138E+10 | -0.05008E-11 | 0.8569106 | 84.35              | 285.241 | 46.668  | 6041   | 1.42 | F0-F1 | F0    | 9.277E+26 | 2.385     | 2.477E+30 | 1.24      |      |   |   |   |  |  |
| 55          | HAT-P-34 b Transit   | 5.453  | 0.0877  | 0.441  | 6.3185E+27 | 3.328 | 1.197 | 0.119104 | Yes | 2.7201E+10 | 4.13144E-11  | 1.1263375 | 87.1               | 303.195 | 18.105  | 6442   | 1.53 | F2-F3 | F2    | 1.393E+27 | 3.580     | 2.737E+30 | 1.38      |      |   |   |   |  |  |
| 56          | WASP-2 b Transit     | 2.719  | 0.0384  | 0.018  | 6.8338E+27 | 3.6   | 1.18  | 0.117613 | Yes | 1.6944E+10 | -4.5371E-11  | 0.7867802 | 85.3               | 3.962   | 1.200   | 6100   | 1.11 | F0-F1 | F0    | 5.893E+26 | 1.515     | 2.208E+30 | 1.11      |      |   |   |   |  |  |
| 57          | WASP-33 b Transit    | 1.220  | 0.02555 |        | 7.7818E+27 | 4.1   | 1.497 | 0.148955 | Yes | 1.521E+10  | 2.44298E-11  | 0.3715679 | 87.67              | 36.713  | 37.550  | 7430   | 1.44 | F8-F9 | F9    | 2.183E+27 | 5.612     | 3.063E+30 | 1.54      |      |   |   |   |  |  |
| 58          | Kepler-25 b Transit  | 12.720 | 0.11    |        | 7.8957E+27 | 4.16  | 0.401 | 0.0399   | Yes | 3.4792E+10 | 1.16377E-10  | 0.4490291 |                    | 286.638 | 39.488  | 6190   | 1.36 | F0-F1 | F1    | 9.381E+26 | 2.411     | 2.480E+30 | 1.25      |      |   |   |   |  |  |
| 59          | HAT-P-16 b Transit   | 2.776  | 0.0413  | 0.036  | 7.9583E+27 | 4.193 | 1.289 | 0.128259 | Yes | 1.8438E+10 | 9.81193E-12  | 0.1809149 | 86.6               | 9.573   | 42.463  | 6158   | 1.24 | F0-F1 | F1    | 7.638E+26 | 1.964     | 2.563E+30 | 1.18      |      |   |   |   |  |  |
| 60          | OGLE-TR-7 b Transit  | 2.486  | 0.0308  |        | 8.541E+27  | 4.5   | 1.61  | 0.180199 | Yes | 2.7315E+10 | -8.85294E-12 | 0.2418148 | 79.8               | 166.980 | -61.146 | 6933   | 1.53 | F6-F7 | F6    | 1.808E+27 | 4.801     | 2.946E+30 | 1.48      |      |   |   |   |  |  |
| 61          | Kepler-21 b Transit  | 42.633 | 0.26    |        | 8.9206E+27 | 4.7   | 0.375 | 0.037113 | Yes | 4.4256E+10 | 3.0664E-10   | 15.570054 |                    | 294.023 | 45.853  | 6340   | 1.22 | F2-F3 | F2    | 8.307E+26 | 2.136     | 2.406E+30 | 1.21      |      |   |   |   |  |  |
| 62          | WASP-14 b Transit    | 2.244  | 0.036   | 0.091  | 1.3933E+28 | 7.341 | 1.281 | 0.127463 | Yes | 1.8063E+10 | -3.6443E-11  | 0.6237463 | 84.32              | 118.276 | 21.895  | 6475   | 1.31 | F2-F3 | F3    | 1.042E+27 | 2.679     | 2.546E+30 | 1.28      |      |   |   |   |  |  |
| 63          | CoRoT-14 b Transit   | 1.512  |         |        | 1.4387E+28 | 7.58  | 1.09  | 0.108458 | No  |            |              | 0         | Not Tidally Locked | 79.6    | 103.424 | -5.536 | 6035 | 1.21  | F0-F1 | F0        | 6.709E+26 | 1.725     | 2.281E+30 | 1.15 |   |   |   |  |  |
| 64          | HAT-P-1 b Transit    | 5.633  | 0.06878 | 0.5171 | 1.7253E+28 | 9.09  | 1.157 | 0.115124 | Yes | 3.1709E+10 | 1.81216E-11  | 0.5746236 | 86.72              | 245.151 | 41.048  | 6450   | 1.75 | F2-F3 | F2    | 1.831E+27 | 4.707     | 2.931E+30 | 1.47      |      |   |   |   |  |  |
| 65          | WASP-18 b Transit    | 0.941  | 0.02026 | 0.0052 | 1.9796E+28 | 10.43 | 1.105 | 0.11592  | Yes | 1.2644E+10 | -9.09368E-12 | 0.1149844 | 86                 | 24.354  | -45.678 | 6400   | 1.23 | F2-F3 | F2    | 8.788E+26 | 2.254     | 2.438E+30 | 1.23      |      |   |   |   |  |  |
| 66          | XO-3 b Transit       | 3.192  | 0.0454  | 0.26   | 2.2177E+28 | 11.79 | 1.217 | 0.121095 | Yes | 2.1461E+10 | -3.8441E-11  | 0.8250384 | 84.2               | 65.470  | 57.817  | 6429   | 1.38 | F2-F3 | F2    | 1.124E+27 | 2.889     | 2.584E+30 | 1.30      |      |   |   |   |  |  |
| 67          | Kepler-20 b Transit  | 6.239  | 0.068   |        | 2.4105E+28 | 12.7  | 0.232 | 0.023085 | Yes | 2.7602E+10 | 7.13424E-11  | 1.5857762 |                    | 296.638 | 39.468  | 6190   | 1.36 | F0-F1 | F1    | 9.381E+26 | 2.411     | 2.480E+30 | 1.25      |      |   |   |   |  |  |
| 68          | Kepler-39 b Transit  | 21.087 | 0.155   | 0.121  | 3.4164E+28 | 18    | 1.22  | 0.121393 | Yes | 4.1835E+10 | 1.04023E-10  | 4.3518122 | 88.83              | 296.960 | 46.034  | 6260   | 1.39 | F0-F1 | F1    | 1.025E+27 | 2.635     | 2.535E+30 | 1.27      |      |   |   |   |  |  |
| 69          | KeCoT-3 b Transit    | 4.257  | 0.057   | 0      | 4.1111E+28 | 21.66 | 1.01  | 0.100498 | Yes | 2.5773E+10 | -2.9184E-11  | 0.6422254 | 85.9               | 292.055 | 0.122   | 6740   | 1.56 | F4-F5 | F4    | 1.735E+27 | 4.460     | 2.892E+30 | 1.45      |      |   |   |   |  |  |
| 70          | KeCoT-1 b Transit    | 1.218  | 0.02466 | 0.0099 | 5.1683E+28 | 27.23 | 1.11  | 0.110448 | Yes | 1.5947E+10 | 2.39743E-11  | 0.3823900 | 87.8               | 0.362   | 39.384  | 6518   | 1.46 | F2-F3 | F3    | 1.329E+27 | 3.417     | 2.706E+30 | 1.36      |      |   |   |   |  |  |
| 71          | KOI 339.01 b Transit | 1.980  | 0.03    |        |            |       |       |          | Yes | 1.2705E+10 | 4.96155E-11  | 0.6303685 |                    | 285.888 | 47.880  | 6013   | 0.87 | F0-F1 | F0    | 3.418E+26 | 0.879     | 1.927E+30 | 0.97      |      |   |   |   |  |  |
| 72          | KOI 339.02 b Transit | 12.834 | 0.105   |        |            |       |       |          | Yes | 2.3525E+10 | 1.73654E-10  | 4.9852083 |                    | 285.888 | 47.880  | 6013   | 0.87 | F0-F1 | F0    | 3.418E+26 | 0.879     | 1.927E+30 | 0.97      |      |   |   |   |  |  |

The data

**Characteristic Timescale/Impact Parameter**, calculated according to the exercise set forth in the section on transit events.

For Excel Code used in the calculations, please see Appendix C.

## 6.4 Summary of Findings

### 6.4.1 What kinds of stars do these planets form around?

#### Spectral Classes of Exoplanetary Stars

|                 |               |                  |
|-----------------|---------------|------------------|
| <b>O : 1</b>    | <b>≤ 0.1%</b> | <b>1/2489</b>    |
| B : 0           | 0%            | 0/2489           |
| A : 8           | 0.3%          | 8/2489           |
| F : 354         | 11.4%         | 354/2489         |
| <b>G : 1378</b> | <b>55.4%</b>  | <b>1378/2489</b> |
| K : 742         | 29.8%         | 742/2489         |
| <b>M : 6</b>    | <b>0.2%</b>   | <b>6/2489</b>    |

*Average Spectral Class : G7V*

*Average Surface Temperature: 5460K*

*Average Stellar Radius: 0.97  $R_{\odot}$*

*Average Stellar Luminosity: 0.96  $L_{\odot}$*

*Average Stellar Mass: 0.92  $M_{\odot}$*

We observe that the most common type of star around which transiting exoplanetary signatures have been detected is the G class main-sequence star, an unsurprising find, considering that our Sun is also of this class. It does seem that there is a hugely disproportionate number of exoplanets (99%) that have been found orbiting the F, G, and K class stars. This is, again, not terribly surprising considering that stars that are either larger or smaller than these types of main sequence stars either are too low mass to have much of a chance of forming planets, or they burn so brightly as to prevent planets from forming from the protoplanetary disc.

However, as history has shown, there is always the potential for exoplanets to pop up in unlikely locations. For example, the single O-class star that was found with an exoplanetary signature was of a rare class of stars known as O-type subdwarfs. These are extremely low-mass stars with a very high surface temperature, and are very unlikely in the population of stars in our galaxy. And yet, this system seems to have an exoplanet in its midst, proving the point, once again, that exoplanets are certainly much more prevalent than once thought. Additionally, the finding of a series of M-class dwarfs with planets orbiting them is also rather surprising, considering the little material that such a system would allow for planet forming.

Ultimately it can be said that the average detected exoplanetary system is a star very much like our Sun in radius, luminosity, and stellar mass, but is perhaps slightly smaller, less luminous, and with a slightly lower surface temperature. However, it is difficult to say if this is simply a result of “Goldilocks syndrome”, that is that G-type stars are simply the perfect combination of size, luminosity, longevity, and prevalence to allow for the easy detection of exoplanets. I suppose the further that the search for exoplanets goes, the more that humanity will be able to decide whether that assumption is correct.

### 6.3.2 Where are these exoplanets located?

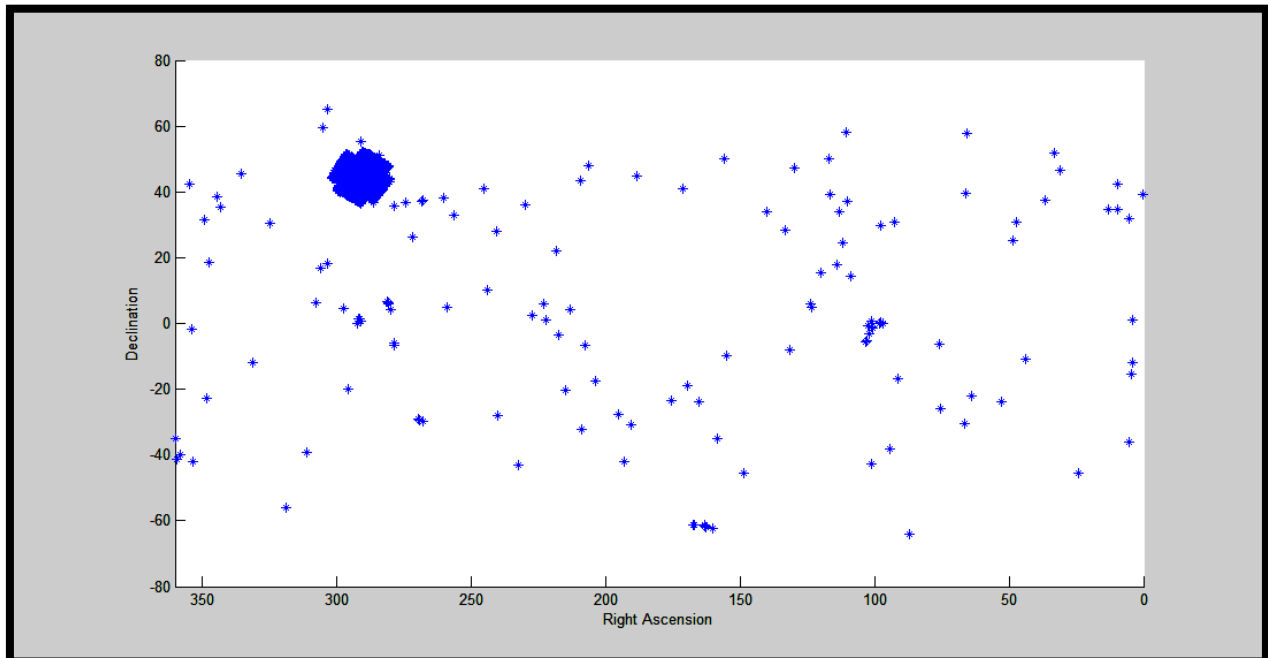


Figure 19: Raw output of the locations of discovered exoplanets. Note the large collection of exoplanets near the top left corner of the plot. These are the discoveries made in the Kepler mission.

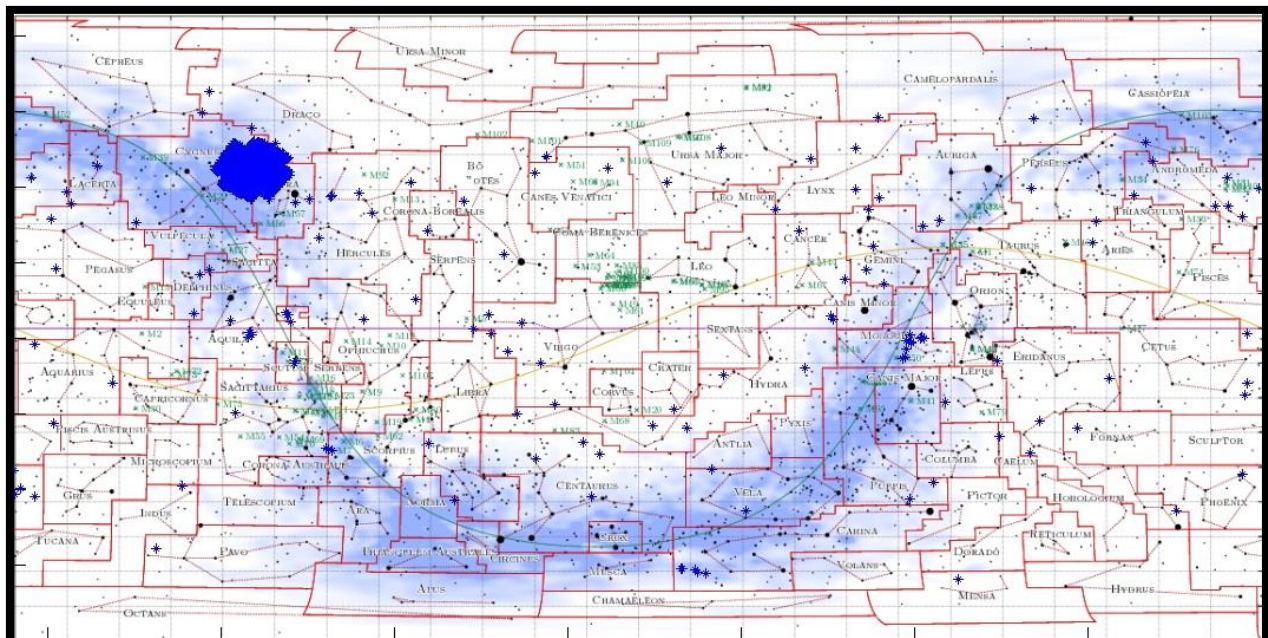


Figure 20: Plot of the data gathered on the locations of exoplanets superimposed on a map of the night sky. Note the Kepler discoveries are found in Cygnus and Lyra, as the mission had described. Otherwise, exoplanetary systems seem to be spread rather evenly throughout the night sky.

## 7. Detecting an Exoplanet

### 7.1 Candidate Selection

The significant information gathered in Stage 2 of the project ultimately provided a very good idea of the locations in the galaxy and the types of stars to look for when detecting exoplanets. As a proof of concept, a previously-discovered exoplanetary system was used as a potential testbed for a future exoplanetary survey based on our findings. Although this extensive survey was not initiated at the time of the observation, it is hoped that the information gathered here will be useful in future endeavors.

The characteristics that were sought in selecting the exoplanetary candidate were defined by our previously-mentioned statistical findings. To summarize, we found that the ideal stellar candidate would possess the following characteristics:

- Main Sequence Single Star
- F, G, or K spectral class
- Roughly the same size, mass, and luminosity as the Sun

Additionally, due to the constraints of detection time, and equipment, it was decided that the exoplanetary candidate system would also possess the following characteristics:

- Short planetary transit cycle (less than 8 hrs, viewable in a single session)
- Brighter than the 12<sup>th</sup> magnitude (to ensure relatively accurate measurements)
- Visible from the observatory's location in the month of April
- Not variable

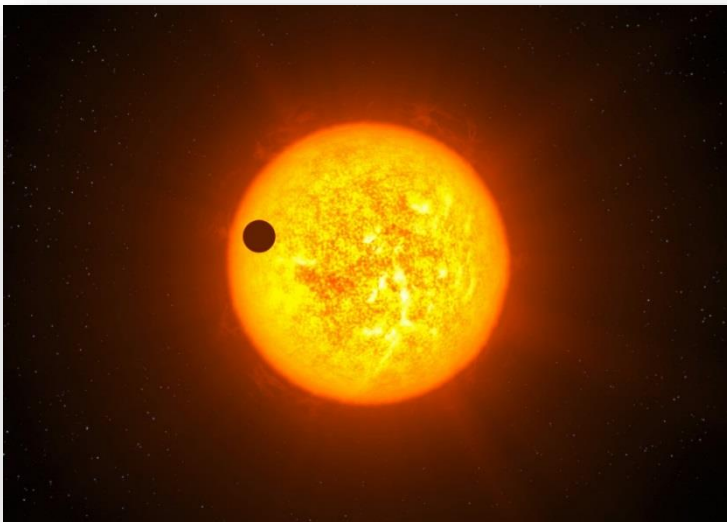


**Figure 21: Artist's impression of the type of exoplanetary system we are looking for: Single G-type main sequence star with a closely orbiting exoplanet near the plane of observation (hence, a short, but observable transit period).**

Ultimately, the exoplanetary system chosen for study was WASP-13, a star located in the constellation Lynx. WASP-13b was an ideal choice for examination because it possessed all of the characteristics which were sought after. The characteristics of the star are listed below.

- ✓ Spectral type: G1V (Main sequence), remarkably similar to our Sun
- ✓ Apparent magnitude: 10.42, Not variable
- ✓ Close to the Celestial Zenith in April
- ✓ Exoplanet orbital period: 4.3 days; transit time: ~300 minutes
- ✓ Negligible eccentricity due to proximity to star, meaning tidally locked
- ✓ Exoplanet orbital inclination = ~85 degrees, transit seen “edge on”

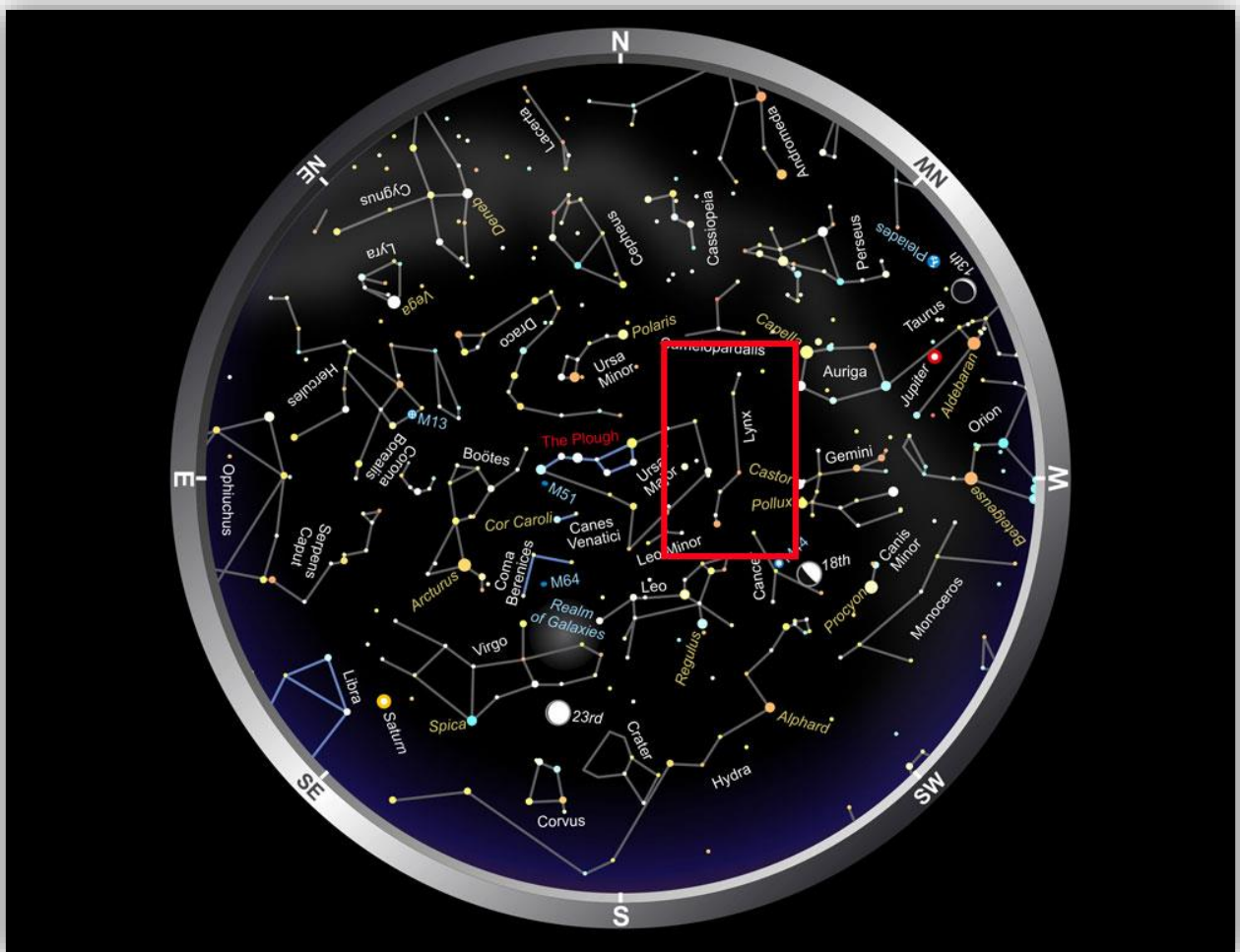
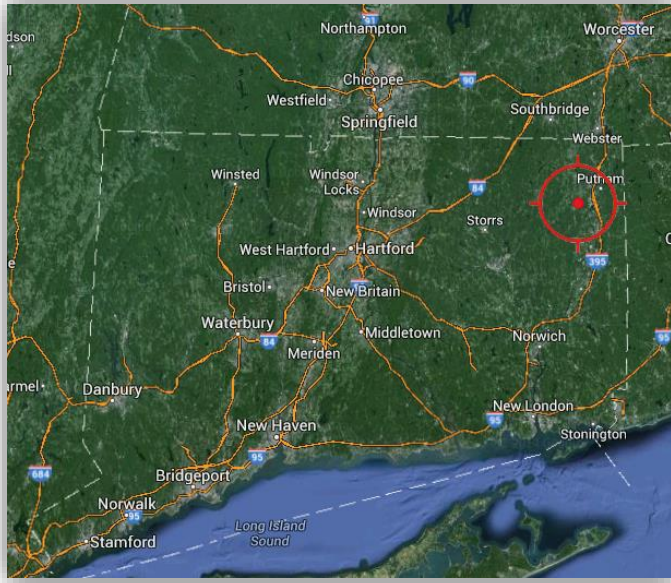


Figure 22: The location of the constellation Lynx in April. Note its proximity to Ursa Major, which dominates the celestial zenith during this month. This ensured that Wasp 13 was easily visible from the observatory during the observation period.

## 7.2 Location and Equipment



**Figure 23: A map of the State of Connecticut highlighting the location of the Olmsted Observatory in Windham County.**

The selected observation site was the Olmsted Observatory, a modest, but well equipped facility located at the Pomfret School in the small town of Pomfret, Connecticut. Located in the rural “Quiet Corner”, this facility is located roughly equidistant from Hartford, Worcester, and Providence, meaning that the effects of light pollution on observations are significantly reduced compared to other suburban locations in the region. Only in far northern New England (such as New Hampshire) could one find darker skies. For most astronomical viewing purposes, these conditions are more than satisfactory.

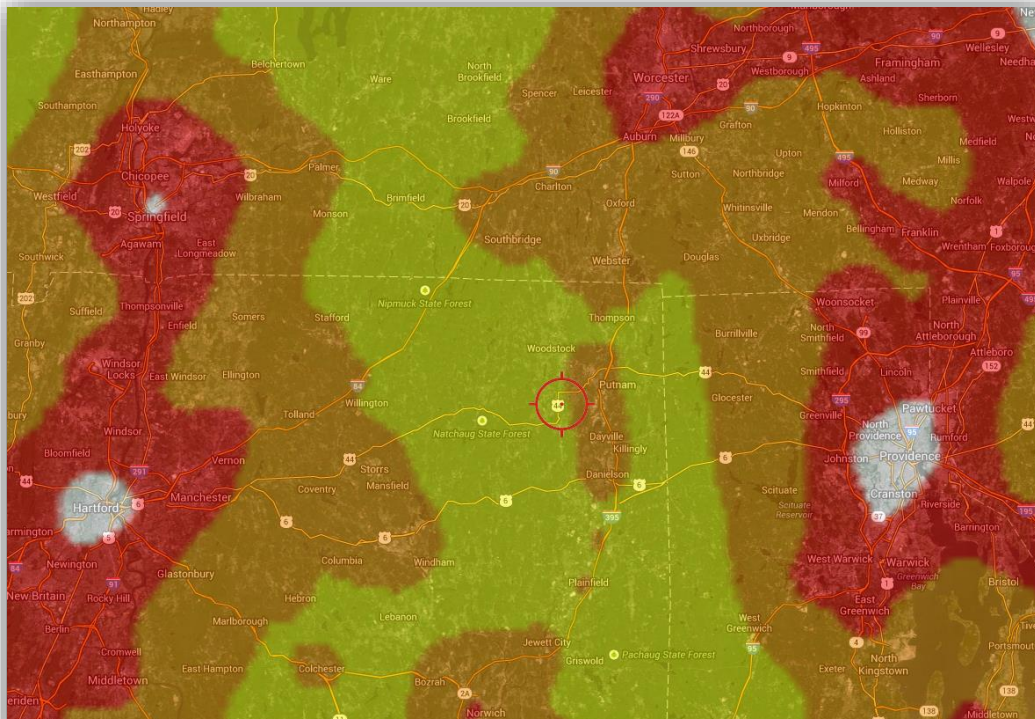


**Figure 24: A light pollution map of the “Quiet Corner” of Northeastern Connecticut from 2001 highlighting the light conditions of the area. White and red denote regions where viewing conditions are poor due to the level of scattered city lights. Orange and yellow regions are considered “fair”, with acceptable levels of light pollution. Green and blue regions (not shown) are considered “excellent” and suffer almost no effects from light pollution. These regions are not found anywhere in Southern New England.**

In addition to reduced light pollution compared to most of Southern New England, the physical location of the Olmsted Observatory on the Pomfret School Campus is also advantageous since it is located next to a soccer field. This provides the observatory with roughly 300 degrees of nearly unobstructed line of sight. While near the backside of the observatory a few tall trees can occasionally prevent the viewing of certain objects, it is almost never a problem, since the observatory's automation software accounts for this automatically. Accounting for distant trees across the field, and the trees in the back, the observatory can observe roughly 15,000 square degrees of the night sky from its present location.

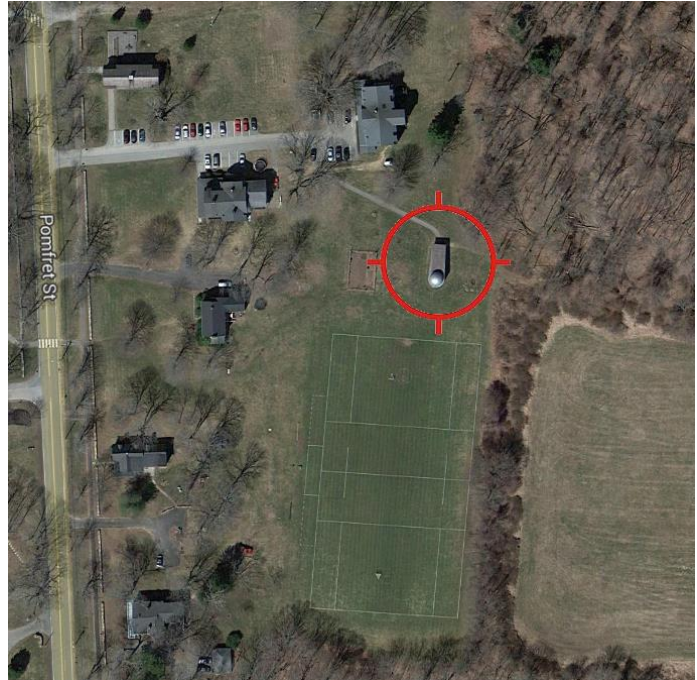


Figure 25: Location of the Olmsted Observatory at Pomfret School

The observatory itself is a small building of roughly 50' x 20' comprised of two levels: a small heated classroom/storage area which is used for astronomy classes, and an observatory dome, which is separated from the main classroom by a set of doors. The lower area is heated in the winter and can be a nice retreat if one has a long observing session. The dome itself is fully automated and can be controlled either remotely or in-person by computer.



Figure 26: The Olmsted Observatory in Spring



**Figure 27: A Celestron /Takahashi setup similar to the one used at the Olmsted Observatory.**

The observational equipment consists of a dual telescope setup consisting of a Celestron 14 Schmidt-Cassegrain main scope coupled with a smaller Takahashi refractor. The two scopes are linked to a supercooled CCD camera which is controlled and regulated by command computer located in the dome. Installed on the command computer are a number of software suites that allow the scopes and the dome to work in tandem to automatically slew to a selected observing location. The whole process of selecting and slewing to a location can be run remotely. Additionally, preset programs may be run to automatically observe or image certain objects at specific times of the night, which can be of great use for both photometric and astrophotographical applications.

### 7.3 Image Capture and Processing

Image capturing and processing was done using a combination of programs, including Pleiades' PixInsight, Cyanogen's MaXIM DL, Software Bisque's The Sky6, and the basic software bundled with the primary CCD controller.

Before observation was conducted, a series of frames were taken to ensure that background noise was removed from the "signal" or image which was trying to be gathered. A "dark frame" was taken once the CCD had been warmed up (but before the mask had been removed), to compensate for the dark noise (unique electrical signature produced by the CCD chip itself). Next, a "bias frame" was taken (with an exposure time of 0) to record any electrical signals that might have interfered with the gathering of a calibrated image. Finally, a "flat frame" was taken after the CCD chip had been exposed to the sky for a period of time. This was meant to equalize the gain of the sensors on the chip so that the sensor "learned" the static components of the environment which it was to be imaging. The flat frame was taken when the night had fallen to maximum darkness (around 90-minutes after sundown). Before imaging, the scope was acclimated in the open air once the dome door had been opened, a period of time which allowed the temperature of the scope and the temperature of the air to equalize. This prevented aberrations caused by moisture buildup and expansion/contraction of the scope's construction materials. With all of these steps completed, it was finally possible to gather a series of calibrated images and photometric readings from the observed object.



**Figure 28:** The starfield in the vicinity of exoplanetary system WASP-13 in Lynx. The star within the green reticule is WASP-13, and the star contained by the red box is the calibration star HD80408. The diffuse objects near the right edge of the image are the distant galaxies NGC 2830 (large elliptical), NGC 2831 (small dot within elliptical), and NGC 2832 (lenticular).

Calibration of magnitude was done by comparing the photometric readings of a nearby star with a stable, known magnitude. In our case, this calibration star was HD80408, a magnitude 8.7 star located less than 10 seconds of arc away. This allowed us to establish the baseline magnitude for WASP-13 before the planet began its transit. Care was taken to ensure that the planet's transit did not occur during the calibration period. Prior to the observation, the WASP-13b transit cycle was calculated and projected based on the series of known transit events observed by previous astronomers. This allowed us to calculate when the next transit event was going to occur: approximately 10:38 EST on April 2, 2013.

## 7.4 Observation Night and Measured Light Curve

The night of April 2, 2013 was cool and clear, with excellent viewing conditions. Calibration procedures commenced at approximately 9:30 PM, and the automatic datapoint collection program was started at 9:45 PM. Image datapoints were set to be gathered at 5-second intervals until the end of the imaging period. During the imaging period, apart from a brief interruption at the start of the cycle due to operator error, there were no events of note and the program was periodically checked to ensure proper functionality during the event. Datapoint collection ended promptly at 11:45 AM, yielding a data collection period of 120 minutes. During this time, 1,357 datapoints were collected.

In order to compensate for small fluctuations in magnitude detection, it was decided that the data would be best represented by binning the 1,357 5-second interval datapoints into averaged 1 minute intervals. By doing this, it was hoped that the datapoints, which were somewhat erratic due to noise, would “average out” and produce a much more readable curve. The 1,357 datapoints were therefore condensed into 113 averaged datapoints, which were then entered into MATLAB to produce the plot seen below.

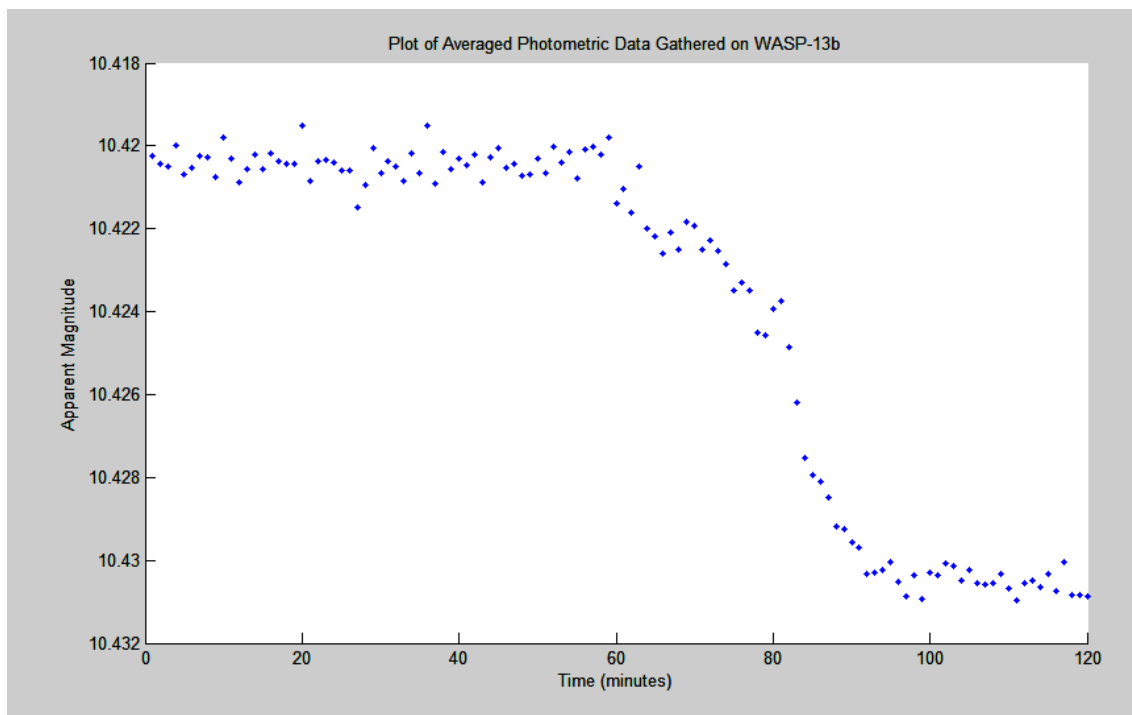


Figure 29: Plot of Averaged Photometric Data Gathered on WASP-13b

## 7.5 Summary of Findings

From the transit curve of WASP-13b, we can gather quite a few pieces of information about the system. Let us assume that we do not initially know much about the WASP-13b system so that we may demonstrate the amount of information that can be learned simply by examining the light curve.

- ✓ First, we observe that the ingress period of the planet is approximately 40 minutes. As we discussed in previous sections of the report, by Keplerian motion, this tells us that the planet's orbital velocity is relatively high, meaning it also must be orbiting close to the star during the transit event. Because of the short period of its transit, and the short period of time between transits (4.3 days), we can say, (based on evidence gathered from our own Solar System and from other exoplanetary systems) that this planet likely has a circular orbit (low eccentricity) and that it is tidally locked.
- ✓ Second, the total drop in magnitude from normal output to transit output was about 0.01 of a magnitude. From this, we can estimate of the ratio of the planet's cross-sectional area compared with its parent star's. If we assume that the star is about 1.5 solar radii, then we can estimate that the total emitting surface of the star WASP-13 is blocked out by the roughly circular "mask" of the WASP-13b planet. If we have an estimate for the size of the stellar disc, then we may gain an estimate for the size of the planet by simply saying that the overall drop in magnitude represents the areal emittance lost due to planetary transit. Therefore, we can find the radius of the planet:

$$\pi R_p^2 = \Delta M * \pi R_s^2$$

$$R_p = \sqrt{\Delta M} * R_s$$

In our case:

$$R_p = (0.1)(1.04 * 10^9 m) = 1.04 * 10^8 m$$

Which is 1.503 times the radius of Jupiter. This compares favorably to the generally accepted value of 1.4  $R_J$  quoted in literature and shows that, although our estimate is not terribly complex, it is in fact fairly accurate.

- ✓ If we analyze the star with a spectrograph to find its surface temperature, we can also use the stellar luminosity formula (which assumes that stars are blackbodies) to calculate the luminosity of the star WASP-13:

$$L_* = 4\pi R_*^2 \sigma T^4$$

Where  $R_*$  is the radius of the star,  $\sigma$  is the Stefan-Boltzmann constant ( $5.67 \times 10^{-8} \text{ W} \cdot \text{m}^{-2} \cdot \text{K}^{-4}$ ), and  $T$  is the surface temperature of the star.

Plugging in for  $T$  and  $R$ , we find the estimated luminosity is:

$$L_* = 9.338 * 10^{26} W$$

Or about 2.4 times the solar luminosity.

Now, by the mass-luminosity relation for main sequence stars:

$$\frac{L}{L_s} = \left( \frac{M}{M_s} \right)^{3.5}$$

We find that the mass of the WASP-13 star will be about 1.28 solar masses.

As we have found even from this simple analysis, there is a great deal of information to be gathered from studying light curves. Further and deeper analysis of light curves and the information that can be gathered from them (including atmospheric analysis) may be found in further literature.<sup>10</sup>

---

<sup>10</sup> Seager, Sara *Exoplanets*. University of Arizona Press (2010).

## 8. Summary and Conclusion

In conclusion, in our grand search for exoplanets, we have covered a great deal of ground. We began by gaining an understanding of the history and development of the science of exoplanets starting in antiquity and ending in the modern era. This provided us with the grand scale of the search and its greater meaning to the scientific community. It also showed us the developments that allowed astronomers and astrophysicists to achieve our current level of understanding.

We then delved into some of the current statistics regarding exoplanetary discoveries and learned about the various techniques that are currently used to detect exoplanets. We also attempted to develop an image of the ideal exoplanetary system by using our statistical data to find the most likely candidate star that might possess an exoplanetary system.

And finally, we used all of the information that we had gathered in sections one and two to influence our decision in the selection of the exoplanetary system WASP-13b in the constellation Lynx, which provided us a direct method for observing and discovering exoplanets of our own. With a successful detection of the exoplanet orbiting this star we have set the ground work for future observations of exoplanets using the aforementioned transit method.

It is hoped that the effort that was put into developing this project will be of use in the future to continue the Search for Exoplanets, and to help this grand science finally discover the “second Earth” which has so long been coveted.

## 9. Appendices

### 9.1 Appendix A – Stellar Development

The principles of Stellar Evolution are a set of topics that could encompass the entirety of a book, but within this appendix I shall provide a brief rundown of the basics behind the formation of stars.

Stellar formation begins within large molecular clouds which dot the starscape of the galaxy. These molecular clouds are made of molecular hydrogen ( $H_2$ ) and other trace materials and are generally found in intricate cloud complexes found in the spiral arms of galaxies.



**Figure 30:** The exquisite barred spiral galaxy NGC 1300 in the constellation Eridanus. Note the bright blue star-forming regions of the spiral arms, indicating the locations of young blue stars and the molecular clouds which spawned them.

When one of these molecular clouds is perturbed (usually by the shockwaves produced by a supernova, or other cataclysmic phenomenon), the molecular hydrogen begins to coalesce, which leads to gravitational compaction in certain regions of the once mostly uniform cloud. The cloud eventually splits into a large collection of smaller, darker, compaction regions, known as Bok globules. The Bok globules found within star-forming nebulae within our galaxy are typically around a light year or two in diameter, and contain all of the necessary ingredients for the formation of new stellar systems.

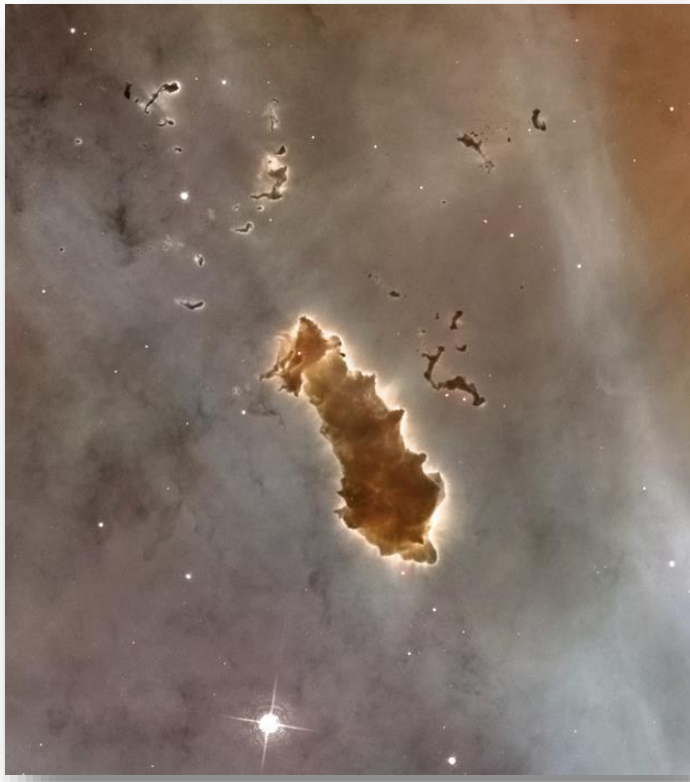


**Figure 31:** A collection of Bok globules in the Carina Nebula (NGC 3372), a star-forming region located about 8,000 light years away.

Although not always the case, further collapse of Bok globules results in the formation of protoplanetary nebulae, also known as proplyds. Proplyds are differentiated from Bok globules in that they are generally smaller (less than a light year across) and that the increased gravitational compaction significantly increases the core temperature of the cloud compared to the surrounding space.

Due to conservation of angular momentum, proplyds begin to take disc shapes relatively early on in their development cycle, and this feature seeks to further differentiate them from the often irregular Bok structures which spawn them.

As the proplyds continue to compact the material at their cores, the center of the disc begins to significantly heat up. Eventually, the core of the proplyd reaches a critical temperature, which then “ignites the spark”, which starts nuclear fusion. When this occurs, the solar wind produced by the newborn star blasts off the remaining dust of the protoplanetary disc.

However, not all material is thrown out in this process. During the formation of the star, chunks of material may accrete outside of the central focus of gravitation, which results in the formation of large bodies of dust, rock, and gas. These chunks eventually coalesce to form into spherical shapes, and are large enough to prevent being blown out by the birth of the new star. These are how planets, comets, asteroids, and other stellar bodies remain in orbit in stellar systems. The evolution of the planetary system throughout its life, however, is a lengthy topic and cannot be fully discussed here.<sup>11</sup>

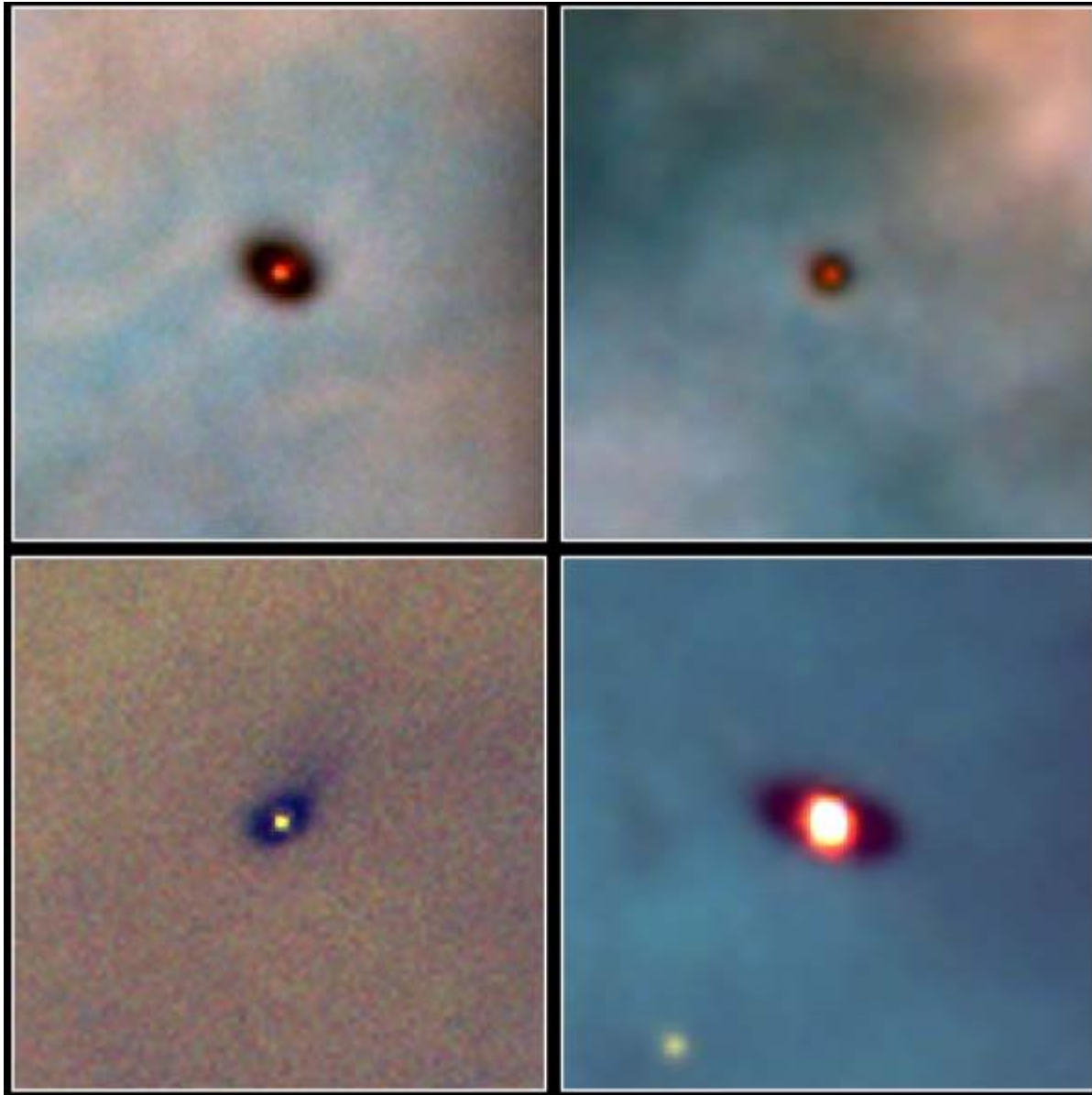


**Figure 32: A series of proplyds at different stages of development found in the Orion Nebula.**

---

<sup>11</sup> For further reading, see: Carroll and Ostlie, *An Introduction to Modern Astrophysics*, 2nd Ed. (2007).

## 9.2 Appendix B – Stellar Classification Systems

Astronomers in previous centuries determined that the vast number of stars in the sky needed classification - a way to organize and categorize stars based on their attributes such as color, brightness, and other, more complex phenomena such as variability. However, it took many years before an all-encompassing, standardized system was to be developed. This section outlines several of the properties used to categorize these different features of stars via observational data.

### Luminosity

Luminosity is defined as the amount of light that a body emits per unit time. Luminosity in astronomy is separated into two distinct categories:

*Apparent:* Referring to only visible light radiation

*Bolometric:* Referring to total EM radiation

As a base point, the Sun's bolometric luminosity is  $3.846 \times 10^{26} W$ . Other stars are generally quoted in multiples of the Sun's luminosity – for example, Sirius A is 25.4 times the Sun's luminosity or  $25.4 L_{\odot}$ .

### Spectral Classes

Stars are classified into spectral classes by the peak wavelength emitted from the surface. This peak wavelength arises from the excitation of certain atoms within the star. The most popular form of classification for spectral class is the Harvard classification system, developed in the early 1900s. This system designates stellar spectra with a letter, O (hottest), B, A, F, G, K, and M (coolest) with each class further divided into subcategories 1-10. For example, our Sun is a G2 type star, denoting a yellowish-white spectral emission 1/5 (2/10) of the temperature of an F type star.

**O-type: Blue-Violet Stars, > 33000K**

**B-type: Blue Stars, 10000-33000K**

**A-Type: Blue-White Stars, 7500-10000K**

**F-Type: Yellow-White Stars, 6000-7500K**

**G-Type: Yellow Stars, 5200-6000K**

**K-Type: Orange Stars, 3700-5200K**

**M-Type: Red Stars, < 3700K**

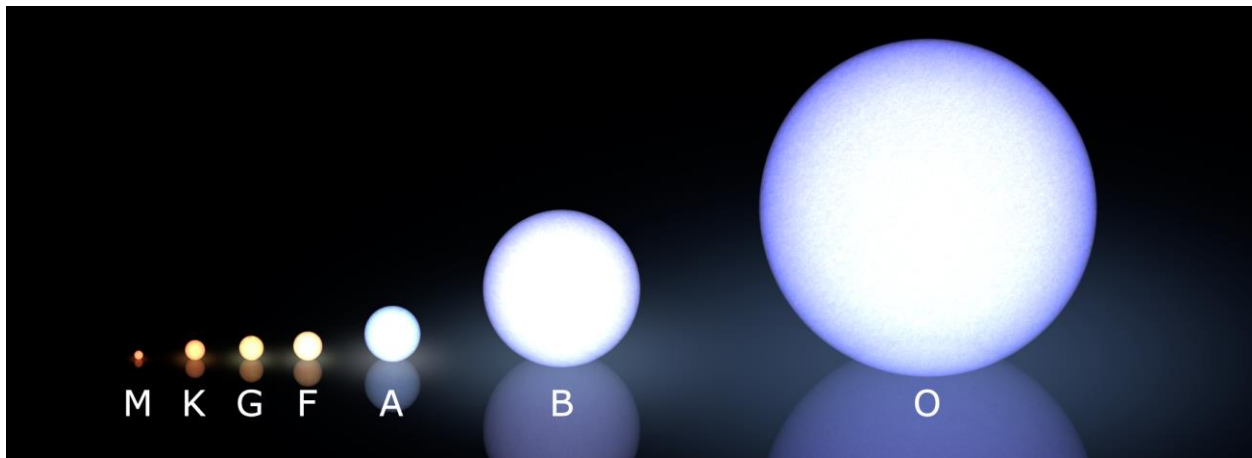


Figure 33: A figure displaying the differences in size of main-sequence stars of each spectral class. Note how much larger a main-sequence O-type star is compared to an M-type.

### The Hertzsprung-Russel Diagram

In 1910, a diagram was developed by Ejnar Hertzsprung and Henry Russel to chart out the distribution of stars based on their spectral classes and luminosities. This diagram, known as the Hertzsprung-Russel diagram, would become the basis for stellar classification and lead to many discoveries pertaining to the nature of stars in the following century. It was found that stars tend to fall within four major categories based on their luminosity and spectral class.

**Main Sequence** – This set corresponds to a long, roughly diagonal line that cuts across the center of the diagram. Stars of this group are in hydrostatic equilibrium and are therefore relatively stable. These stars are given the Roman numeral designation V (dwarfs).

**Giants** – This group corresponds to a set above the main sequence, although they tend to occupy only the F-M spectral classes. As main sequence stars age, they diminish in spectral class and therefore end up in the giants cluster. Ambiguity sometimes occurs in the O-B types as stars in this region could also be considered main-sequence. These stars are given the Roman numeral designations II (bright giants), III (giants), and IV (sub-giants).

**Supergiants** - Similar to the giants cluster, the supergiants cluster results mainly from large main sequence stars shifting through the spectral classes as they age. There can occasionally be difficulty in defining a supergiant, as large stars with B or O type spectral classes could also be considered main sequence stars despite being several times the mass of the Sun. These stars are given the Roman numeral designation I (supergiants).

**White dwarfs and other sub-dwarfs** – White and sub-dwarfs correspond to a large cluster of low luminosity stars of all spectra on the H-R diagram. White dwarfs are formed from the collapse of main sequence stars and are characterized by low luminosity, but an early spectral

class, such as A or F. However, a large portion of these sub-dwarfs are red dwarfs, a star type that makes up over 70% of all stars in the galaxy. These are, in fact, main sequence stars that are very small and have very low luminosity. These occupy the lower-right corner of the diagram. Stars of this category are given the Roman numeral designations VI (sub-dwarfs) and VII (white dwarfs).

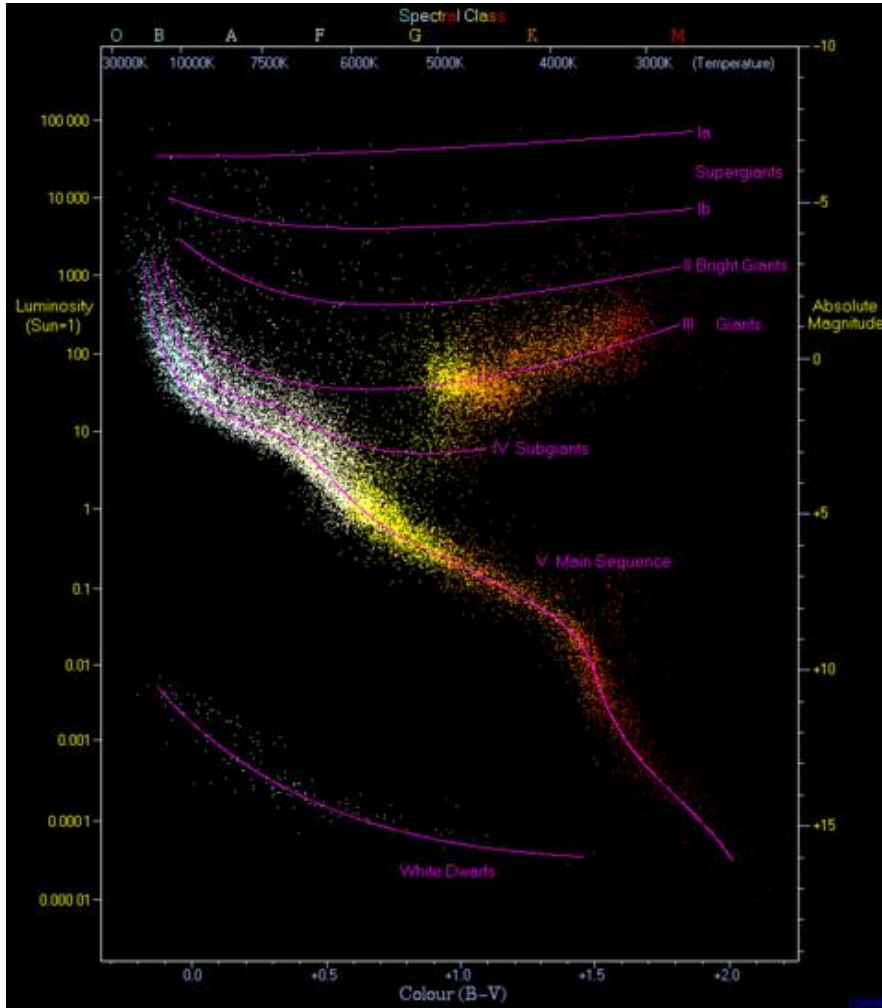


Figure 34: A representation of the Hertzsprung-Russel diagram

### Peculiarities in the Hertzsprung-Russel Diagram

#### The Hertzsprung Gap

One of the main features within the H-R diagram is a rift that exists between the main sequence and the giants regions between the A and G spectral classes and the -1 to +3 luminosity values. The reason for this gap arises from the fact that when stars age, they spend a very short amount of time in this transition zone.

## The Instability Strip

The previously mentioned Hertzsprung Gap is also the lower limit of what is known as the instability strip: a region which extends upwards through the Giant and Supergiant phases. This instability arises from a specific combination of luminosity and spectral class, which causes the star to pulsate. There are a wide variety of variable stars within this strip, including T Tauri, ZX Virginis and the famous Cepheid variable.

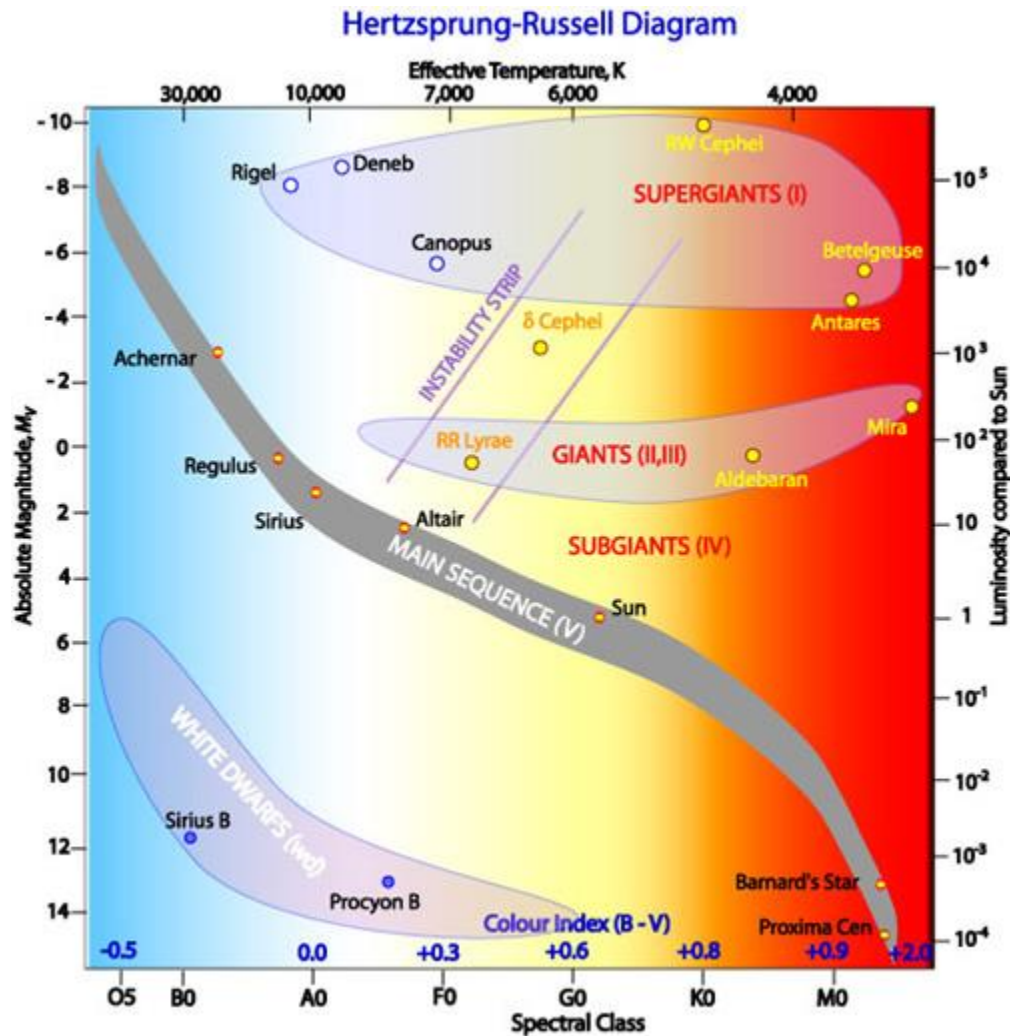


Figure 35: A Hertzsprung-Russell diagram displaying the instability strip

## 9.3 Appendix C - Excel Algorithms

### Base Spectral Class (sample):

=IF(AND(Q2>=2000,Q2<=3500),"M",IF(AND(Q2>3500,Q2<=5200),"K",IF(AND(Q2>5200,Q2<=6000),"G",IF(AND(Q2>6000,Q2<=7500),"F",IF(AND(Q2>7500,Q2<=10000),"A",IF(AND(Q2>7500,Q2<=10000),"B",IF(AND(Q2>10000,Q2<=33000),"O", "Z"))))))))

=IF(AND(Q2>7500,Q2<=8000),"A0-A1",IF(AND(Q2>8000,Q2<=8500),"A2-A3",IF(AND(Q2>8500,Q2<=9000),"A4-A5",IF(AND(Q2>9000,Q2<=9500),"A6-A7",IF(AND(Q2>9500,Q2<=10000),"A8-A9")))))

=IF(AND(Q2>=7500,Q2<=7750),"A0",IF(AND(Q2>=7750,Q2<=8000),"A1"))

### Luminosity:

=4\*PI()\* (R2\*6.963\*10^8)^2\*(5.67\*10^-8)\*Q2^4

### Mass:

=IF(S2="M", (W2/0.23)^(1/2.3)\*(1.99\*10^30), IF(OR(S2="K", S2="G", S2="F", S2="A"), (W2)^(1/4)\*(1.99\*10^30), IF(OR(S2="B", S2="O"), ((W2)^(1/3.5)/1.5)\*(1.99\*10^30), "ERROR"))

**Characteristic Timescale:** =(R3\*6.95\*10^8)\*(C3/(PI()\*D3))

**Impact Parameter:** =(D3\*COS(N3))/(R3\*6.95\*10^8)

**Tidal Locking:** =IF(AND(D4>=0.001, D4<=0.6), "Yes", "No")

**Transit Period:** =IF(J4="Yes", ABS(L4\*K4), "Not Tidally Locked")

*\* Raw Excel sheets available upon request.*

## 10. Acknowledgements

In completing this project, there are two people who I would like to thank in the utmost for their unwavering assistance and continued support in this effort.

**Professor P.K. Aravind**, *Worcester Polytechnic Institute* - my advisor, whose unwavering loyalty and steady guidance helped me to see this project through to the very end, and who was always there to render assistance in my time of need. To him I owe many thanks, far more than I could ever give.

-and-

**Josh Lake**, *The Pomfret School* - director of Pomfret's Olmsted Observatory, who taught me everything I know about observatory automation, imaging software, and so much more, and who graciously allowed me the opportunity to use the observatory whenever I needed it. To him, I also owe many thanks.



## Table of Figures

|  |    |
|--|----|
| FIGURE 1: A PLOT OF THE ORBITAL DISTANCE AND SIZE PARAMETERS FOR A SELECTION OF EXOPLANETARY DISCOVERIES HIGHLIGHTING THE VARIOUS METHODS USED IN THEIR DETECTION. BLUE DOTS REPRESENT DISCOVERIES MADE USING THE RADIAL VELOCITY TECHNIQUE, GREEN DOTS REPRESENT DISCOVERIES MADE USING THE TRANSIT METHOD. NOTE HOW THE VAST MAJORITY OF DISCOVERIES MADE WERE ACHIEVED USING THESE TWO METHODS. | 21 |
| FIGURE 2: SIMPLE GRAPHIC EXHIBITING THE “WOBBLING” MOTION OF A STAR AROUND ITS BARYCENTER DUE TO THE PRESENCE OF A PLANET.   | 22 |
| FIGURE 3: A SIMPLE GRAPHIC ILLUSTRATING THE CONCEPT OF WAVEFRONT COMPRESSION AND EXPANSION AS OBSERVED IN THE DOPPLER EFFECT AND THE SUBSEQUENT VISUAL EFFECT THAT IT HAS ON WAVELENGTH.   | 23 |
| FIGURE 4: A DIAGRAM COMBINING THE TWO PREVIOUS IDEAS TO SHOW THE PRINCIPLES OF THE RADIAL VELOCITY METHOD.   | 24 |
| FIGURE 5: A DIAGRAM DISPLAYING THE PHOTOMETRIC LIGHT CURVES GATHERED FROM A NUMBER OF DIFFERENT PLANETS FROM THE KEPLER EXOPLANETARY SURVEY MISSION. NOTE, THE RATIOS OF THE PLANETS TO THE STARS AND THE MAXIMUM DEPTH OF THE LIGHT CURVE.  | 26 |
| FIGURE 6: A SAMPLE LIGHT CURVE GATHERED FOR THE HYPOTHETICAL “EXOPLANET A”   | 27 |
| FIGURE 7: VENUS TRANSITING THE SUN. NOTE HOW DARK THE DISC OF THE PLANET IS IN COMPARISON TO THE SUN’S EMITTING SURFACE. ONE CAN SEE, HOWEVER, THE EFFECT THAT THE ATMOSPHERE HAS – THE THICK, DIFFUSE ATMOSPHERE SCATTERS AND REFLECTS.   | 29 |
| FIGURE 8: GRAPHIC EXPLAINING THE VARIOUS PARAMETERS IN THE DERIVATION OF TRANSIT TIME PROBLEM.   | 30 |
| FIGURE 9: KEPLER’S PRINCIPLE OF “SWEEPING OUT EQUAL AREAS IN EQUAL TIMES”  | 31 |
| FIGURE 10: A SIMPLE COMPARISON OF PLANETS WITH CIRCULAR AND HIGHLY ECCENTRIC ORBITS. PLANETS WITH HIGH ECCENTRICITIES MAY BE MISLEADING BECAUSE THEIR ORBITAL VELOCITIES WILL BE HIGH FOR A SHORT TIME WHILE THEY ARE NEAR THEIR PARENT STAR, BUT VERY SLOW ELSEWHERE.   | 32 |
| FIGURE 11: THE SUN AND VENUS, FEATURING “LIMB DARKENING” – THE BROWNING OF THE SUN’S COLOR NEAR THE EDGES OF THE DISC. THIS CONTRIBUTES LESS AT LONG DISTANCES, BUT STILL REQUIRES CORRECTION ALGORITHMS IN SENSITIVE ANALYSES.  | 33 |
| FIGURE 12: A DIAGRAM EXHIBITING THE BASIC PROCESS OF THE PULSAR TIMING METHOD.   | 34 |
| FIGURE 13: ONE OF THE MOST FAMOUS IMAGES FEATURING GRAVITATIONAL LENSING – GALAXY CLUSTER ABELL 2218. NOTE THE “FISHEYE EFFECT” NEAR THE CENTER OF THE IMAGE CAUSED BY THE EXTREME COMBINED MASS OF SEVERAL LARGE GALAXIES IN THE FOREGROUND.  | 35 |

- FIGURE 14: EXOPLANETS AROUND FOMALHAUT DIRECTLY IMAGED USING A VORTEX CORONAGRAPH. NOTE THE MASK USED TO BLOCK OUT THE BLINDING RAYS OF THE STAR TO ALLOW THE PLANETS TO BE OBSERVED. 36
- FIGURE 15: A SIMPLE ILLUSTRATION SHOWING THE BASIC IDEA BEHIND ASTROMETRY. 37
- FIGURE 16: RAW OUTPUT OF THE LOCATIONS OF DISCOVERED EXOPLANETS. NOTE THE LARGE COLLECTION OF EXOPLANETS NEAR THE TOP LEFT CORNER OF THE PLOT. THESE ARE THE DISCOVERIES MADE IN THE KEPLER MISSION. 43
- FIGURE 17: PLOT OF THE DATA GATHERED ON THE LOCATIONS OF EXOPLANETS SUPERIMPOSED ON A MAP OF THE NIGHT SKY. NOTE THE KEPLER DISCOVERIES ARE FOUND IN CYGNUS AND LYRA, AS THE MISSION HAD DESCRIBED. OTHERWISE, EXOPLANETARY SYSTEMS SEEM TO BE SPREAD RATHER EVENLY THROUGHOUT THE NIGHT SKY. 43
- FIGURE 18: ARTIST'S IMPRESSION OF THE TYPE OF EXOPLANETARY SYSTEM WE ARE LOOKING FOR: SINGLE G-TYPE MAIN SEQUENCE STAR WITH A CLOSELY ORBITING EXOPLANET NEAR THE PLANE OF OBSERVATION (HENCE, A SHORT, BUT OBSERVABLE TRANSIT PERIOD). 44
- FIGURE 19: THE LOCATION OF THE CONSTELLATION LYNX IN APRIL. NOTE ITS PROXIMITY TO URSA MAJOR, WHICH DOMINATES THE CELESTIAL ZENITH DURING THIS MONTH. THIS ENSURED THAT WASP 13 WAS EASILY VISIBLE FROM THE OBSERVATORY DURING THE OBSERVATION PERIOD. 45
- FIGURE 20: A MAP OF THE STATE OF CONNECTICUT HIGHLIGHTING THE LOCATION OF THE OLMSTED OBSERVATORY IN WINDHAM COUNTY. 46
- FIGURE 21: A LIGHT POLLUTION MAP OF THE “QUIET CORNER” OF NORTHEASTERN CONNECTICUT FROM 2001 HIGHLIGHTING THE LIGHT CONDITIONS OF THE AREA. WHITE AND RED DENOTE REGIONS WHERE VIEWING CONDITIONS ARE POOR DUE TO THE LEVEL OF SCATTERED CITY LIGHTS. ORANGE AND YELLOW REGIONS ARE CONSIDERED “FAIR”, WITH ACCEPTABLE LEVELS OF LIGHT POLLUTION. GREEN AND BLUE REGIONS (NOT SHOWN) ARE CONSIDERED “EXCELLENT” AND SUFFER ALMOST NO EFFECTS FROM LIGHT POLLUTION. THESE REGIONS ARE NOT FOUND ANYWHERE IN SOUTHERN NEW ENGLAND. 46
- FIGURE 22: LOCATION OF THE OLMSTED OBSERVATORY AT POMFRET SCHOOL 47
- FIGURE 23: THE OLMSTED OBSERVATORY IN SPRING 47
- FIGURE 24: A CELESTRON /TAKAHASHI SETUP SIMILAR TO THE ONE USED AT THE OLMSTED OBSERVATORY. 48
- FIGURE 25: THE STARFIELD IN THE VICINITY OF EXOPLANETARY SYSTEM WASP-13 IN LYNX. THE STAR WITHIN THE GREEN RETICULE IS WASP-13, AND THE STAR CONTAINED BY THE RED BOX IS THE CALIBRATION STAR HD80408. THE DIFFUSE OBJECTS NEAR THE RIGHT EDGE OF THE IMAGE ARE THE DISTANT GALAXIES NGC 2830 (LARGE ELLIPTICAL), NGC 2831 (SMALL DOT WITHIN ELLIPTICAL), AND NGC 2832 (LENTICULAR). 50
- FIGURE 26: PLOT OF AVERAGED PHOTOMETRIC DATA GATHERED ON WASP-13B 51
- FIGURE 27: THE EXQUISITE BARRED SPIRAL GALAXY NGC 1300 IN THE CONSTELLATION ERIDANUS. NOTE THE BRIGHT BLUE STAR-FORMING REGIONS OF THE SPIRAL ARMS,

|  |    |
|--|----|
| INDICATING THE LOCATIONS OF YOUNG BLUE STARS AND THE MOLECULAR CLOUDS WHICH SPAWNED THEM.  | 55 |
| FIGURE 28: A COLLECTION OF BOK GLOBULES IN THE CARINA NEBULA (NGC 3372), A STAR-FORMING REGION LOCATED ABOUT 8,000 LIGHT YEARS AWAY.   | 56 |
| FIGURE 29: A SERIES OF PROPLYDS AT DIFFERENT STAGES OF DEVELOPMENT FOUND IN THE ORION NEBULA.  | 57 |
| FIGURE 30: A FIGURE DISPLAYING THE DIFFERENCES IN SIZE OF MAIN-SEQUENCE STARS OF EACH SPECTRAL CLASS. NOTE HOW MUCH LARGER A MAIN-SEQUENCE O-TYPE STAR IS COMPARED TO AN M-TYPE. | 59 |
| FIGURE 31: A REPRESENTATION OF THE HERTZSPRUNG-RUSSEL DIAGRAM  | 60 |
| FIGURE 32: A HERTZSPRUNG-RUSSEL DIAGRAM DISPLAYING THE INSTABILITY STRIP   | 61 |

\*For a complete list of figure sources, please contact the author of this paper.

## References

- Wolfczcan and Fran. *A planetary system around millisecond pulsar PSR 1257+12*. Nature (1992)
- Mayor, M. & Queloz, D. *A Jupiter-mass companion to a solar-type star*. Nature 378, 355-359 (1995)
- Marcy, Geoffrey W. et al. *Three New 51 Pegasi-Type Planets*. The Astrophysical Journal 474 (1997).
- Rivera, Eugenio J. et al. *The Lick-Carnegie Exoplanet Survey: A Uranus-mass Fourth Planet for GJ 876* (2010)
- Kalas, Paul; et al. *Optical Images of an Exosolar Planet 25 Light-Years from Earth*. Science 322. (2008)
- Dumusque et al. *An Earth mass planet orbiting Alpha Centauri B*. Nature 490. (2012)
- de Pater and Lissauer. *Planetary Sciences*, Cambridge University Press. (2001).
- Seager, Sara. *Exoplanets*. University of Arizona Press. (2010)
- Carroll and Ostlie. *An Introduction to Modern Astrophysics*. 2nd Ed. Pearson (2007).